Title

Analysis of the ubiquitin-modified proteome identifies novel host determinants of Kaposi's sarcoma herpesvirus lytic reactivation

Authors

Amerria Causey[1], Mathew Constantine[1], Arie Admon[3], Alfredo Garzino-Demo[2] and Elana Ehrlich[1]

Institutions

(1) Biological Sciences, Towson University, Towson, Maryland, United States

(2) Dept. of Molecular Medicine, University of Padova, Padova, Italy, Dept of Microbiology and Immunology, University of Maryland School of Medicine, Baltimore, MD, USA

(3) Biology, Technion - Israel Institute of Technology, Haifa, Israel

Abstract

Kaposi's Sarcoma Herpesvirus (KSHV) is the causative agent of Kaposi's Sarcoma (KS) and is associated with primary effusion lymphoma (PEL), multicentric Castleman's disease (MCD) and two inflammatory diseases. KSHV-associated cancers are primarily associated with genes expressed during latency, while other pathologies are associated with lytic gene expression. The major lytic switch of the virus, RTA, interacts with cellular machinery to co-opt the host ubiquitin proteasome system to evade the immune response as well as activate the program of lytic replication. Through SILAC labeling, ubiquitin remnant enrichment and mass spectrometry, we have analyzed the RTA dependent ubiquitin-modified proteome. We identified RTA dependent changes in the populations of polyubiquitin chains, as well as changes in ubiquitinated proteins in both cells expressing RTA and naturally infected cells following lytic reactivation. We observed an enrichment of proteins that are also reported to be SUMOylated, suggesting that RTA, a SUMO targeting ubiquitin ligase, may function to alleviate a SUMO dependent block to lytic reactivation. In addition, we report an RTA dependent mechanism of immune evasion, targeting TAP dependent peptide transport resulting in decreased HLA complex stability. The results of this analysis increase our understanding of mechanisms governing the latent to lytic transition in addition to the identification of a novel RTA dependent mechanism of immune evasion.

Introduction

Kaposi's Sarcoma Herpesvirus (KSHV), also known as HHV-8, is the causative agent of Kaposi's Sarcoma (KS) and is associated with primary effusion lymphoma (PEL) and multicentric Castleman's disease (MCD)[1,2]. KSHV is also linked to the inflammatory diseases, KSHV inflammatory cytokine syndrome and immune reconstitution syndrome-KS [3–5]. KSHV is classified as a Group 1 carcinogen by the International Agency for Research on Cancer and the National Toxicology Program 14th Report on Carcinogens [6].

KSHV, a gamma herpesvirus, has a two-phase lifecycle consisting of latency and lytic replication. During latency, few genes are expressed, and genome replication occurs with the purpose of segregation to daughter cells during cell division. Lytic replication is initiated via expression of the viral Regulator of Transcription Activation (RTA) protein. This results in rapid expression of lytic genes, replication of viral DNA, assembly of virus particles and egress from the cell [7].

KSHV is primarily found in cells as a latent infection. Initiation of KSHV-associated cancers is, in part, associated with the genes expressed during latency, which maintain an environment that allows for the survival of cells harboring latent virus. To maintain a latent infection, several checkpoints and mechanisms of regulation are bypassed to progress through the cell cycle without triggering apoptosis, autophagy or an antiviral response. Dysregulation of such critical processes as cell cycle control, apoptosis and immune response-related signaling pathways are believed to be associated with development of an oncogenic environment. In addition to virus propagation and proliferation, lytic gene expression is also thought to be required for tumorigenesis in KS and MCD. In PEL, most cells express latent genes, with 1-5% of cells exhibiting spontaneous reactivation and lytic gene expression[7].

The mechanisms responsible for lytic reactivation in natural infection are unclear, however chemical inducers of lytic reactivation such as phorbol esters and histone deacetylase inhibitors have been utilized to study the lytic program of gene expression and more recently cell lines harboring latent virus and doxycycline inducible RTA provide a more specific model for the study of reactivation [8,9]. Aside from being the major switch for reactivation of KSHV from latency, RTA has been assigned intrinsic ubiquitin ligase activity and has been shown to recruit cellular ubiquitination machinery, ubiquitin ligases and deubiquitinases[10,11]. RTA has also been designated a SUMO targeting ubiquitin ligase, specifically targeting SUMO2/3 modified proteins for proteasomal degradation[12,13]. RTA targets IRF7 for proteasomal degradation as a mechanism to abrogate the interferon α/β response to viral infection[11]. In addition, RTA is reported to degrade a number of known RTA repressors such as ID2, MyD88, Hey1, LANA and NFκB (p65)[14–18]. This E3 ubiquitin ligase activity has been mapped to a Cys/His- rich domain between amino acids 118 and 207 of RTA[11]. RTA was also shown to recruit and stabilize a cellular ubiquitin ligase, RAUL, via recruitment of the deubiquitinating enzyme HAUSP[10]. We have previously reported RTA induced degradation of vFLIP through the cellular E3 ligase Itch [19,20].

We hypothesized that identification of additional substrates targeted for ubiquitination by RTA would provide insight into novel mechanisms of regulation of the latent-lytic transition. To this end, we carried out a comparative proteomics analysis in both RTA transfected 293T cells and TREX BCBL-1 RTA SILAC labeled cells. We identified 66 ubiquitination sites in 40 proteins shared between both data sets, representing proteins with RTA induced ubiquitination alterations in BCBL-1 cells. We validated 27.5% of the proteins for RTA dependent degradation in the context of a CURE (course-based undergraduate research experience). SUMO 2/3 was identified as a target of RTA induced ubiquitination. Our dataset was enriched with proteins that are also known to be SUMOylated, with more than a third of the proteins in the matched dataset also reported to be SUMOylated according to PhosphoSitePlus. Inhibition of SUMOylation resulted in increased

production of infectious virus, supporting a role for RTA induced degradation of SUMO in the transition to lytic replication. We observed RTA dependent degradation of proteins associated with MHC class I antigen presentation and provide evidence supporting a novel mechanism of immune evasion associated with decreased TAP transport and intracellular HLA and proteasome subunit degradation. This mechanism, along with the well-established activities of the K3 and K5 KSHV encoded ubiquitin ligases in MHC class I endocytosis, represent a multipronged attack on antigen presentation by KSHV during lytic replication and presumably contribute to the success of the virus in establishing a lifelong infection.

Methods

Cell Lines, Plasmids, Transfection, and Antibodies

HEK 293T, iSLK, and BAC16 iSLK were cultured in DMEM medium supplemented with 10% BS and TRex BCBL-1 cells were maintained in RPMI supplemented with 20% FBS. Cells were grown at 37°C with 5% CO_2. The following plasmids were used in this study: FLAG tagged ORFs in pcDNA3.1+/C-(K)DYK were purchased from Genscript: CDK1 (NM_001786.5), PSMB3 (NM_002795.4), H2AFX (NM_002105.3), HSPA1A (NM_005345.6), TOLLIP (NM_019009.4), RPS3 (NM_001005.5), MCM7 (NM_005916.5), VDAC1(NM_003374.3). HLAC (NM_002117.5) was obtained from Genecopoeia in a Gateway PLUS Shuttle clone and cloned into pcDNA-DEST40 (ThermoScientific). Flag tagged SUMO 2/3 and RTA were provided by Diane and Gary Hayward. Cells were transfected using PEI (Polyethylenimine, Linear, MW 25000, Transfection Grade, Polysciences) at a ratio of 3ul/1ug plasmid DNA. The following antibodies were used in this study: BACTIN (sc-69879V5), V5 (sc-271944) from Santa Cruz Biotech, FLAG M2 from Sigma Aldrich, FITC labeled HLA-ABC Antibody (11-9983-42 Invitrogen), PE Mouse Anti-Human CD184 (Clone 12G5, BD), and RTA antibody was provided by Gary Hayward.

Ubiquitin-modified proteome analysis

Proteomics experiments were conducted in collaboration with the Smoler Proteomics Center at the Technion-Israel Institute of Technology. Experiments were carried out using doxycycline inducible TREx BCBL1 RTA cells and 293T cells transfected with RTA or pcDNA control vector. Cells were maintained as described above. Prior to ubiquitin remnant motif K-ε-Gly-Gly (KGG) purification, cells were acclimated in SILAC media (lysine and arginine deficient media supplemented with stable isotope containing lysine and arginine ("heavy" media contained $^{13}C_6$ $^{15}N_4$ Arg and $^{13}C_6{}^{15}N_2$ Lys)) for 7 days and evaluated for efficient SILAC labeling [21]. RTA expression was induced in TREx BCBL1 RTA cells via addition of doxycycline (1μg/ml) to cells for 24 and/or 48h as indicated. 293T cells were transfected with RTA or empty vector pcDNA 3.1 and harvested following 48h incubation. Cells were treated with 10μM MG132 6 h prior to harvesting. Cell pellets were washed with PBS and flash frozen in liquid nitrogen. Cells were lysed in 8M urea 400mM ammonium bicarbonate buffer pH 8, sonicated and cleared of cell debris by centrifugation. 2mg protein was processed for peptide purification by reducing with DTT (30min at 60°C, 3mM final concentration), cysteines were alkylated with 10mM idoacetamide, followed by trypsin digest (0.1μg/5ug protein) overnight. Following desalting by reverse phase chromatography on SepPac disposable cartridges (Waters), peptides containing the ubiquitin remnant motif – K-ε-Gly-Gly were enriched via incubation with anti-K-ε-Gly-Gly antibody-bound agarose beads. Peptides were eluted with 0.2% TFA. Eluted peptides were desalted using C18 stage tips and dried prior to analysis via LC-MS/MS.

The peptides were resolved by reverse-phase chromatography on 0.075 X 180-mm fused silica capillaries (J&W) packed with Reprosil reversed phase material (Dr Maisch GmbH, Germany). The peptides were eluted with linear 180 minutes gradient of 5 to 28% 15 minutes gradient of 28

to 95% and 25 minutes at 95% acetonitrile with 0.1% formic acid in water at flow rates of 0.15 µl/min. Mass spectrometry was performed by Q Executive HFX mass spectrometer (Thermo) in a positive mode using repetitively full MS scan followed by collision induces dissociation (HCD) of the 30 most dominant ions selected from the first MS scan.
MS raw data was processed using MaxQuant software followed by identification of proteins using the Andromeda peptide search engine to search against the HHV8 and human UniProt databases (Uniprot-proteome 27.7.18 (73101 entries), Uniprot-proteome HHV8) [22,23]. Data merging and statistical analysis was done using the Perseus[24]. Functional enrichment analysis was performed using DAVID (https://david.ncifcrf.gov/) and STRING (https://string-db.org/). Final data set was curated by matching the data from the TREx BCBL1 RTA dataset with the data from the 293T cell dataset to identify the RTA dependent ubiquitin-modified proteome. For time course proteomics experiments cells were cultured in the absence of MG132, lysates were separated on a 12% polyacrylamide gel and peptides extracted from Coomassie stained gel slices using in-gel digest and processed for LC-MS/MS without KGG purification. Experiments were performed in triplicate with a reverse SILAC labeling control, replicates with the highest Pearson's correlation coefficient were used for the final data analysis.

Transfection
Cells were transfected at 60-70% confluence using 1µg/ml polyethyleneimine (PEI) linear, MW~25,000 at a ratio of 1µg plasmid DNA:3µl PEI. After 15 min of incubation at room temperature the mixture was added to the cells. 24 h post transfection the media was changed and if appropriate, 2.5µM of MG132, 5µM of Chloroquine, or 2µM of Cycloheximide was added.

SDS-PAGE and Western Blot Analysis
Cells lysates were prepared by direct addition of 2X Laemmli buffer. Lysates were separated using a 4%-20% ExpressPlus PAGE Gel (Genescript) and MOPS running buffer. Proteins were transferred to a PVDF membrane using Trans-Blot Turbo using the Bio-Rad defined program for 1.5 mm gels. Membranes were blocked in 5% non-fat dry milk in PBS for 1 h followed by incubation with primary antibody overnight at 4°C and secondary antibody for 1 h at room temperature. Proteins were visualized by addition of ECL substrate and detection of chemiluminescence using a Licor C-DiGit or Azure 300.

TAP Peptide Transport Assay
iSLK cells were treated with 1ug/ml doxycycline at 90% confluence to induce RTA expression. 48 hrs post doxycycline induction, cells were harvested, partially permeabilized and incubated with a peptide pool. Peptide pool contained the following cysteine AF 488 modified peptides at a concentration of 10nM: NST-F (RRYQNST[C]L), C4-F (RRY[C]KSTEL), and R9 (EPGY[C]NSTD). Cells were incubated with 10mM ATP or ADP for 30 minutes at either 37°C or on ice. Cells were washed 3x with PBS before being fixed with 2% paraformaldehyde and analyzed using a Guava EasyCyte Flow cytometer.

Surface and Intracellular Flow Cytometry
Cells were dissociated with 0.25% trypsin (Life Technologies) and resuspended in FACS wash buffer. Cells were washed twice, permeabilized (for intracellular staining only) and then incubated or directly incubated (surface staining only) with FITC labled MHC ABC antibody (Invitrogen) or PE labled CXCR4 (BD Biosciences) at 4°C for 30 minutes. Cells were washed 3 times with FACS buffer at 4°C and analyzed using a Guava EasyCyte Flow cytometer.

SEAP Assay
Vero rKSHV.294 and 293T MSR tet-OFF cells were kindly provided by David Lucak[25]. Day one: Vero rKSHV.294 were plated in a six-well plate and treated with 2-D08, DMSO, or NaBr where

indicated. Day two: 293T MSR tet-OFF cells were plated in a six-well plate. Day three: media from 293T MSR tet-OFF cells was replaced with virus containing media from the rKSHV.294 cells. Day five: 25 μl of media was harvested and heat inactivated at 65°C for 30 minutes. SEAP activity was quantified using the Great EscAPe SEAP assay (Clontech). Fluorescence was read on a Filtermax F5 plate reader (Molecular Devices).

Results

Characterization of the RTA dependent KSHV ubiquitin-modified proteome.

Given that RTA is the master lytic switch and has been shown to not only have intrinsic ubiquitin ligase and SUMO targeting ubiquitin ligase activity but is also reported to interact with cellular components of the ubiquitin proteasome system, we reasoned that identification of host proteins that displayed RTA dependent differential ubiquitination would increase our understanding of the latent to lytic transition. KSHV encodes two ubiquitin ligases (K3 and K5) that are expressed during lytic replication; however, our goal was to identify RTA specific targets.

To identify targets of RTA induced differential ubiquitination, we designed our workflow in two disparate cell lines, doxycycline inducible TREx BCBL1 RTA cells, which contain the entire viral genome, and RTA transfected 293T cells, which contain RTA only, with the rationale that the matched datasets would yield RTA specific targets. Cells were adapted to SILAC media as follows: light media contained “light” lysine and arginine and heavy media contained “heavy” lysine (13C6;15N2) and arginine (13C6;15N4) amino acids based on the protocol of Ong and Mann, 2007[21]. Following confirmation of stable labeling, cells were either treated with doxycycline to induce RTA expression or transfected with RTA or vector control. Cells were either harvested for proteomics to evaluate lytic induction and protein abundance or treated with MG132 and incubated with anti-K-ε-Gly-Gly antibody-bound agarose to isolate peptides containing ubiquitin remnants. Ubiquitinated peptides were enriched with anti-K-ε-GG antibody, followed by processing for mass spectrometry on a Q-Exactive HF-X Hybrid Quadrupole-Orbitrap Mass Spectrometer. For proteomics, to evaluate protein abundance, cells were harvested at the indicated time points, and lysates processed for MS. Data was analyzed using MaxQuant and Perseus (Fig.1).

Time-course of lytic induction.

A proteomics experiment was first conducted in TREx BCBL1 RTA cells to assess lytic gene expression over a 24h time-course. Peptides of viral origin displayed an increase in peptides of lytic protein origin as well as a sustained presence of other proteins such as LANA and vIL6 (Fig. 2a and 2b). RTA expression was confirmed in transfected 293T cells (Fig. 2c). In TREx BCBL-1 RTA cells, analysis of peptides of cellular origin revealed a decrease in the detection of proteins previously reported to be degraded following lytic induction (Fig. 2d). HLA-A/ HLA-B or MHC class I is known to be downregulated via the action of viral encoded ubiquitin ligases K3 and K5[26–28]. We also observed a decrease in BST2/Tetherin, also reported to be downregulated by K5 via endocytosis and subsequent downregulation in the endosome[29]. SPN/leukosialin was also significantly downregulated but has not been described previously. We also observed a modest but significant (q=0.012285714) increase in Integrin alpha-6. This was interesting due to the involvement of integrins in cytomegalovirus entry and induction of angiogenesis (Fig. 2e)[30,31].

Ubiquitin-modified proteome analysis in RTA transfected and naturally infected cells.

Analysis of anti-K-ε-GG enriched ubiquitinated peptides resulted in the identification of 193 differentially ubiquitinated sites in 151 proteins in cells transfected with RTA, and 272 sites in 211 proteins in doxycycline treated TREx BCBL1 RTA cells. Sixty-six of these sites in 40 proteins

were shared between both data sets, representing proteins with RTA induced ubiquitination alterations in BCBL-1 cells (Fig. 3a-b). Experiments were performed in triplicate and the experiments with the highest Pearson correlation coefficient (293T RTA r=0.97 and TRExBCBL-1 RTA r=0.68) were used for further analysis (Fig. 3 c-d). While we observed greater variability within the TREx BCBL-1 RTA experiment, we did observe an overall similar trend in the behavior of a large number of ubiquitination sites in both cell lines (Fig 3 b, e, and f).
STRING analysis of proteins displaying an RTA dependent decrease in ubiquitination revealed two functional groups of proteins (Fig. 4a). One cluster is involved in DNA damage repair and the other is associated with ubiquitin binding. Analysis of proteins with increased ubiquitination in RTA expressing cells relative to control indicated functional clusters of proteins involved in diverse cellular processes including antigen presentation, DNA replication, DNA damage repair, cell cycle, SUMOylation, translation, transcription, and the proteasome (Fig 4b)[32]. Gene-annotation enrichment analysis using DAVID resulted in clustering into functional groups [33,34]. The groups with the lowest Benjamini values are included in Fig 4c. We also observed an increase in K48 and K63 linked polyubiquitin chains in transfected 293T cells as well as a significant increase in ubiquitination of SUMO 2/3 in the matched dataset (Fig 4d, 6a). These observations are consistent with the reported functions of RTA as a ubiquitin ligase, manipulator of the ubiquitin proteasome system and SUMO targeting ubiquitin ligase [10–12,20].

Evaluation of the stability of selected cellular proteins in the presence of RTA.
To validate the results of our proteomics experiment, in collaboration undergraduate students participating in a CURE (course-based undergraduate research experience), we selected 11 proteins based on student generated hypotheses to evaluate protein stability in the presence of RTA expression (Table 1). Tagged ORFs were expressed in 293T cells and evaluated for stability in the presence of RTA or pcDNA vector control. The following proteins that displayed increased ubiquitination in the ubiquitin-modified proteome screen, exhibited decreased stability in the presence of RTA: HLA-C, CDK1, PSMB3, HSPA1A, TAP2, RPS3, MCM7, VDAC1 and SUMO2/3 (Fig 5 a-c, e, g-k). Both H2AX and TOLLIP displayed decreased ubiquitination in the presence of RTA. Monoubiquitination of H2AX is associated with DNA damage response signaling, therefore, we would not expect to observe changes in protein stability, and we did not observe significant reductions in H2AX protein levels (Fig 5 d). Interestingly, TOLLIP displayed decreased ubiquitination in cells expressing RTA, however we observed a dramatic decrease in protein levels in the presence of RTA compared to vector controls (Fig 5 f). In addition to being a negative regulator of IL-1 and Toll-like receptor signaling, TOLLIP also functions as an adaptor, connecting ubiquitinated cargo to autophagosomes. This observation warrants further exploration since KSHV is known to dysregulate autophagy[35,36].

RTA targets SUMO2/3 for ubiquitination and degradation.
RTA is a well characterized SUMO targeting ubiquitin ligase (STUbL), therefore it was not surprising when SUMO 2/3 was identified as highly ubiquitinated at K11 and K45 (range 1.3-2.9 H/L ratio) in RTA expressing 293T and doxycycline induced TREx BCBL-1 RTA cells (Fig 6a). Further analysis of the ubiquitin-modified proteome dataset suggests that the RTA induced, or lytic, ubiquitin-modified proteome is enriched for proteins that are SUMOylated. The human proteome contains approximately 12,434 proteins that are ubiquitinated, of those proteins, 2,434 or 19.5% are also reported to be SUMOylated, however within the RTA dependent ubiquitin-modified proteome 30.7% (TREx BCBL-1), 38.3% (293T), and 34.4% (matched matrix) of the proteins are also SUMOylated (Fig 6b). In fact, 61.5% of the proteins from the matched matrix that localize to the nucleus are reported to be SUMOylated. This observation suggests that the STUbL activity of RTA may be partly responsible for the observed increase in ubiquitinated proteins, specifically in the nuclear compartment. RTA is known to have intrinsic ubiquitin ligase activity as well as interact with cellular ubiquitin ligases and these, in addition to indirect

mechanisms, may account for the remaining ubiquitination observed.

The RTA dependent degradation of SUMO 2/3 is dose dependent (Fig 6c); however, it is unclear whether degradation is occurring via the proteasome or lysosome/autophagosome as treatment with MG132 or chloroquine failed to stabilize these ubiquitin-like modifiers (Fig 6d). SUMOylation appears to play a significant role in maintaining latency, as inhibition of SUMOylation resulted in increased production of infectious virus as quantified by secreted alkaline phosphatase assay (Fig. 6e). We utilized Vero rKSHV.294 cells that contain a reporter gene that expresses secreted placental alkaline phosphatase (SeAP) from a tetracycline responsive promoter. SeAP is secreted into the media only after successful infection of 293 MSR Tet OFF cells. Vero rKSHV.294 cells were treated with increasing concentrations of 2-D08. After 48h incubation, virus containing media was collected and added to 293 MSR Tet OFF cells. Media was assayed for SeAP activity following 72h incubation. We observed a significant dose dependent increase ($p<0.0001$) in SeAP activity at concentrations of 30 μM and higher. RTA expression reduced the half-life of SUMO 2/3 monomer and conjugates as evidenced by cycloheximide chase (Fig. 6f). These data suggest that RTA targets SUMO 2/3 for degradation and that SUMOylation is important for maintaining latency in Vero rKSHV.294 cells.

RTA targets antigen presentation through diverse mechanisms.

Analysis of the ubiquitin-modified proteome yielded three proteins that are associated with antigen presentation: HLA (A, B and C), TAP2, and PSMB3. These three proteins play a role in antigen processing and presentation (Fig 7a). We initially observed HLA A and B downregulation in our time course experiment (Fig 2d). While KSHV K3 and K5 are known to downregulate MHC class I via endocytosis[37], ubiquitination was observed in RTA transfected 293T cells in addition to doxycycline treated TREx BCBL-1 cells, suggesting that there may be an additional RTA dependent mechanism for HLA downregulation. TAP2 is an ABC transporter that, in complex with TAP1, participates in the transport of proteasome generated peptides from the cytosol to the endoplasmic reticulum for loading onto nascent MHC class I (HLA) molecules. The TAP1-TAP2 peptide transport complex is targeted by multiple viruses, serving as an effective mechanism of immune evasion. TAP2 is reported to interact with Epstein Barr virus BLNF2a, herpes simplex virus US12/ICP47, and adenovirus E3-19K[38–41]. We observed TAP2 ubiquitination at K356 which is located within the peptide binding loop. PSMB3 is a subunit of the proteasome and is one of many proteasome subunits that we identified in our dataset. We observed RTA dependent degradation of HLA following 24h RTA expression (Fig 5a). This degradation was dose dependent with RTA reducing HLA half-life to 2h post cycloheximide addition compared to 6h in empty vector transfected cells (Fig. 7b and c). Similarly, we observed a decrease in PSMB3 and TAP2 abundance (Fig 5 c and g, respectively) in RTA transfected 293T cells. Degradation of PSMB3 was proteasome dependent and occurred with a rapid RTA dependent decrease in protein half-life (Fig. 8 a-c).

Based on these observations, we hypothesized that peptide transport was being inhibited, either through inhibition of TAP2 or a structural effect on proteasome function. To evaluate this hypothesis, we employed a peptide transport assay based on the method described by Fishbach et al. [42]. This assay utilized a peptide pool containing FITC labeled peptides. Doxycycline inducible iSLK RTA cells lacking BAC16 were subjected to mild permeabilization and incubated with peptide pools under the indicated conditions. Following 30 min incubation, cells were washed, and peptide translocation was quantified by flow cytometry detection of FITC. We observed translocation of peptides into the ER in iSLK cells incubated at 37°C in the presence of ATP, however cells with doxycycline induced RTA expression displayed decreased peptide translocation, suggesting that RTA is interfering with TAP dependent transport of peptides into the ER either directly or indirectly through interference with proteasome function (Fig 9a-b). Proteins that are not properly folded are targeted for degradation by ERAD. Specifically, HLA

molecules that fail to bind β-2-microglobulin or peptide are retrotranslocated, ubiquitinated and degraded [43]. Mass spectrometry analysis of HLA ubiquitination induced by β-2-microglobulin depletion identified two luminal lysines, K200 and K267[44]. We observed RTA induced ubiquitination of HLA-B and C on K200. If inhibition of peptide transport and subsequent degradation via ERAD were to occur, we would expect to see decreased intracellular staining of HLA. iSLK cells lacking BAC16 were treated with doxycycline or media control followed by staining for endogenous intracellular HLA A, B, and C or CXCR5 as a control. RTA expressing cells displayed significantly decreased (9-fold average decrease in mean fluorescence intensity) intracellular HLA staining compared to untreated controls. There was no impact on the unrelated receptor CXCR5 (Fig 9c-d). Taken together these data supports the model that KSHV RTA targets antigen presentation through inhibition of peptide import into the ER resulting in a decrease in intracellular HLA abundance.

Discussion

RTA is the primary regulator of the latent to lytic transition in KSHV. RTA is not only the transcriptional transactivator responsible for the activation of lytic gene expression, but also has ubiquitin ligase activity and is known to both directly and indirectly target proteins of viral and cellular origin for ubiquitination. Many of the targets of RTA induced degradation represent repressors of lytic reactivation. Targets of RTA include SMC5/6, ID2, SUMO 2/3, vFLIP, IRF7, MyD88, Hey1, LANA and NFκB (p65) [10,12,14,16–18,20,45–47] Using the rationale that RTA targets repressors of lytic reactivation we set out to identify novel regulators of the latent to lytic transition using a proteomics-based approach. We utilized SILAC labeling and ubiquitin remnant enrichment to identify proteins that display RTA dependent differential ubiquitination. We observed an RTA dependent increase in K-48 and K-63 linked polyubiquitin chains. We identified 40 proteins that displayed RTA dependent differential ubiquitination. These proteins function in cellular processes including DNA damage repair, transcriptional regulation, DNA replication, apoptosis, and immune evasion.

Through the development of a course-based undergraduate research experience, designed to provide authentic research experiences to diverse populations of undergraduate students, we selected proteins to validate. Students selected proteins, generated hypotheses, and validated degradation of HLA-C, Cdk-1, PSMB3, HSPA1A, TOLLIP, TAP2, RPS3, MCM7, VDAC1, and SUMO2/3. H2AX displayed RTA dependent decreased ubiquitination in our ubiquitin-modified proteome dataset and was not significantly degraded as observed by western blot. Viral replication often disturbs the nuclear structure, chromatin, and/or produces nucleic acid intermediates that activate the DNA damage response (DDR) pathway. Viruses have evolved to either utilize components of the DDR pathway or target the pathway to prevent the potential outcomes of apoptosis and/or cell cycle arrest. H2AX is phosphorylated in response to double strand breaks and acts to recruit repair proteins to sites of damage. In KSHV infection, H2AX is phosphorylated and latently expressed LANA utilizes phospho-H2AX to maintain the viral episome[48,49]. This interaction is thought to be important for maintaining latency. Monoubiquitination of H2AX at K120 has been shown to be important for assembly of DDR factors [50]. H2AX has also been observed in the periphery of viral replication centers[51]. It is possible that deubiquitination of H2AX in the presence of RTA promotes lytic replication by disassembling DDR complexes so they can be recruited to viral replication centers. Perhaps this is a mechanism to disrupt the interaction of the viral genome with LANA and host chromatin during lytic reactivation. Future studies will evaluate these hypotheses.

Here we present two observations: 1. the degradation of SUMOylated proteins to promote lytic replication and 2. the inhibition of antigen presentation through abrogation of peptide transport into the ER. RTA is a well characterized STUbL, so it was not surprising when we observed SUMO

2/3 to be among the most highly ubiquitinated proteins identified in our RTA dependent ubiquitin-modified proteome[12]. In fact, our ubiquitin-modified proteome was enriched for ubiquitinated proteins that are reported as SUMOylated via Phosphosite Plus, often on the same lysine. When we analyzed the SUMOylation status and cellular localization of the proteins that displayed an RTA dependent increase in ubiquitination, we found that 72.3% of the of the proteins that were also SUMOylated are localized to the nucleus. RTA is primarily localized to the nucleus. Taken together, this observation supports a model where nuclear localized RTA targets SUMOylated proteins to promote lytic reactivation. To probe the functional role of SUMOylation in maintaining latency we utilized the infectivity assay developed by the Viera and Lucak labs[25,52] When Vero rKSHV.294 cells, containing virus with the gene encoding secreted alkaline phosphatase, were treated with increasing doses of a small molecule inhibitor of SUMOylation, we observed a dose dependent increase in production of infectious virus. These data are consistent with reports that RTA STUbL activity is required for lytic reactivation and gene expression [12].

KSHV encoded ubiquitin ligases K3 and K5 play an important role in immune evasion via ubiquitination and subsequent endocytosis of HLA[37]. We observed increased ubiquitination of HLA in both doxycycline induced TREx BCBL-1 RTA and RTA transfected 293T cells in addition to decreased levels of peptides of HLA origin in TREx BCBL-1 cells as early as 12hrs post lytic induction. Ubiquitination and subsequent degradation of HLA-C was observed in RTA transfected 293T cells, suggesting an additional K3/K5 independent mechanism of HLA targeted immune evasion. DNA viruses have evolved diverse mechanisms to target antigen presentation, frequently targeting the TAP peptide transporter. Herpesviruses in particular frequently target TAP function. Cytomegalovirus US6 targets TAP by inhibiting ATP binding[40,53]. HSV-1 ICP47 inhibits peptide transport by blocking the peptide-binding site and EBV interferes with both peptide and ATP binding [38,41]. We observed TAP2 ubiquitination at K356 which is located within the peptide binding loop[54]. Expression of RTA in iSLK cells resulted in reduced peptide transport. We also observed rapid destabilization of PSMB3, a proteasome subunit. The exact mechanism of inhibition of peptide transport remains unclear. Potential mechanisms include RTA induced degradation of TAP2 or ubiquitination of TAP2, resulting in decreased peptide binding.

RTA is primarily localized to the nucleus. This begs the question – how is RTA targeting cytoplasmic proteins. 13/29 of the proteins that displayed increased ubiquitination are nuclear, however what about the 16 that are cytoplasmic? RTA is translated in the cytoplasm and imported into the nucleus. It is possible that some activity occurs prior to nuclear import or that a subset of RTA localizes to the cytoplasm. This model is supported by our observation that the RTA has the largest impact on HLA stability 24h post transfection/doxycycline induction, with a decreased effect at 48h when RTA has presumably localized to the nucleus. Alternatively, RTA may be exerting its effects on cytoplasmic proteins indirectly, either through increasing expression of cellular ubiquitin ligases or destabilizing a deubiquitinase that is both nuclear and cytoplasmic. In the case of TAP2, this complex is localized to the ER membrane. The ER membrane is contiguous with the nuclear envelope, increasing the potential for interactions while the RTA is being imported into the nucleus. It is likely that aside from the SUMO targeting activity of RTA, one model will not explain how all proteins are targeted and this remains an area for future research.

Taken together, here we have identified 40 proteins that display RTA dependent differential ubiquitination. We validated 27.5% of the proteins for RTA dependent degradation. Our dataset was enriched with proteins that are also known to be SUMOylated. Inhibition of SUMOylation resulted in increased production of infectious virus, supporting a role for RTA induced degradation of SUMO and SUMOylated proteins in the transition from latency to lytic replication. We observed RTA dependent degradation of proteins associated with MHC class I antigen presentation and provide evidence supporting a novel mechanism of immune evasion associated with decreased

TAP dependent peptide transport and increased intracellular HLA and proteasome subunit degradation. This report contributes to our understanding of KSHV biology by identifying new points of virus-host interaction and describing a novel mechanism of immune evasion by KSHV RTA during lytic replication that likely contributes to the success of the virus in establishing a lifelong infection. Future study of the RTA targets identified in this study have the potential to further our understanding of the latent to lytic transition and lead to the identification of new chemotherapeutics.

Figure legends

Figure 1. Schematic describing experimental design for comparative proteomics analysis. Experiments were carried out in both TREx BCBL1 RTA and RTA transfected 293T cells. Cells were grown in SILAC media containing heavy or light lysine and arginine, supplemented with dialyzed FBS. Cells were treated with MG132 6h prior to harvest. 25ug of protein was saved for proteomic analyses following preparation of tryptic peptides. Tryptic peptides were enriched for ubiquitin remnants with anti-K-ε-GG antibody, followed by processing for mass spectrometry. Data was analyzed using Maxquant and Perseus. Created with Biorender.com

Figure 2. Time-course of lytic induction. (a-b) Doxycycline induced lytic reactivation of TREx BCBL1 RTA cells resulted in an increase in peptides derived from lytic proteins (viral peptides noted in green in b) and a decrease in peptides of cellular protein origin (cellular proteins of interest noted in red and HLA indicated in blue) (c) RTA transfected 293T cells expressed RTA (d) Peptides of cellular origin previously reported to be downregulated following lytic induction. (e) Integrin alpha 6 displayed a modest increase. TREx BCBL1 RTA cells were treated with doxycycline (1ug/ml) for 0, 4, 8, 16, and 24h. 293T cells were transfected with RTA using PEI. $1.8x10^7$ cells were harvested in an 8M Urea buffer. 6ug of protein was reduced, alkylated, trypsin digested, cleaned on C18 stage tips and processed for MS. Data was analyzed using Maxquant, Perseus, and Graphpad Prism.

Figure 3. Analysis of the ubiquitin-modified proteome in RTA transfected and KSHV infected cells. (a) Venn diagram illustrating the number of proteins that displayed increased and decreased ubiquitination in each dataset and shared following filtering in Perseus. (b) Heat map displaying shared ubiquitination sites between RTA transfected and KSHV infected cells. Duplicate experiments displayed for each cell type. Red=H/L ratio >0.5, Green=H/L ratio <0.5 (c-d). Scatterplots demonstrating reproducibility between experiments with Pearson correlation coefficient. (c) 293T RTA (d) TREx BCBL-1 RTA. (e) Percent coefficient of variation within each dataset. (f) Shared ubiquitination site scatterplot rank vs log_2 H/L ratio. Demonstrating behavior of each modification in each dataset. Log_2 H/L ratio >0.5, <-0.5 were considered significant increase or decrease respectively. Blue=TREx BCBL-1 RTA, Orange=293T RTA

Figure 4. RTA expression induced alterations in the ubiquitome of 293T and BCBL1 cells. (a-b) STRING analysis of proteins that displayed at least a 0.5 fold (a) decrease or (b) increase (Log_2H/L ratio) in ubiquitination in the matched (BCBL1 and 293T) dataset. (c) DAVID analysis of matched dataset. (d) K63 and K48 linked polyubiquitin chains were increased in RTA expressing 293T cells ((Log_2H/L ratio = 0.57 and 1.49, respectively).

Table 1. List of proteins selected for validation by CURE class.

Figure 5. Validation of latent/lytic ubiquitin-modified proteome data. 293T cells were transfected with the indicated expression vectors in the absence or presence of RTA. Lysates were analyzed by immunoblot against the indicated epitope tags, RTA, or B-actin as a loading control.

Figure 6. RTA targets SUMO 2/3 for degradation. (a) SUMO 2/3 displayed increased ubiquitination in both doxycycline induced BCBL-1 cells and RTA transfected 293T cells (Log_2 H/L ratio) (b) The KSHV latent/lytic ubiquitin-modified proteome is enriched for proteins that are also SUMOylated. Proteins were evaluated for evidence of SUMOylation via PhosphoSitePlus. (c) RTA induced degradation of SUMO 2/3 is dose dependent. Increasing amounts of RTA were co-transfected with 1μg FLAG-SUMO2/3. Lysates were analyzed as indicated below. (d) RTA induced degradation of SUMO 2/3 occurs via diverse mechanisms. 293T cells were transfected with SUMO2/3 plus RTA or vector control where indicated. Lysates were treated with 10μM MG132 or 5μM of Chloroquine 5h prior to harvesting (e) Inhibition of SUMOylation results in lytic reactivation. Vero rKSHV.294 cells that contain a SeAP reporter gene were treated with increasing concentrations of SUMOylation inhibitor 2-D08. Following 48h incubation, virus containing media was collected and added to 293 MSR Tet OFF cells. Media was assayed for SeAP activity following 72h incubation. (f) Cyclohexamide chase illustrating RTA dependent reduction of SUMO 2/3 the half-life. 293T cells were transfected with Flag tagged SUMO 2/3 with or without RTA or empty vector control where indicated. Lysates were analyzed by SDS-PAGE followed by immunoblot against Flag-SUMO2/3, RTA, or BACTIN as a loading control. Protein half-life was graphed using a representative western blot and image J. SUMO 2/3 monomer bands were normalized to BACTIN bands and graphed relative to time 0, -RTA control using Graphpad Prism.

Figure 7. RTA targets antigen presentation by targeting PSMB3, TAP2, and HLA. (a) Hypothesis: RTA targets ER associated HLA by inhibiting TAP2 and PSMB3. Created with Biorender.com (b) RTA induces a dose dependent degradation of HLA-C. Increasing amounts of RTA were cotransfected with V5 tagged HLA-C. HLA-C stability was analyzed by SDS PAGE followed by immunoblot against V5, RTA, and BACTIN (c) Cycloheximide chase to evaluate HLA half-life. 293T cells were transfected with HLA with RTA or empty vector control. 24h following transfection cycloheximide was added and cells were harvested at the indicated timepoints and analyzed by SDS PAGE and immunoblot followed by densitometry using ImageJ. Graph is based on one representative experiment of three replicates. HLA bands are normalized to BACTIN bands and graphed relative to -RTA time 0 control.

Figure 8. RTA induced the rapid proteasomal degradation of PSMB3. (a) RTA induces the proteasomal degradation of PSMB3. 293T cells were transfected with PSMB3 with RTA or empty vector control. 48h following transfection cells were treated with MG132, chloroquine or control DMSO for 5 hours. Cells were harvested at the indicated timepoints and analyzed by SDS PAGE and immunoblot. (b-c) Cycloheximide chase to evaluate PSMB3 half-life. 293T cells were transfected with PSMB3 with RTA or empty vector control. 16h following transfection cycloheximide was added and cells were harvested at the indicated timepoints and analyzed by SDS PAGE and immunoblot followed by densitometry using ImageJ. Graph is based on one representative experiment of three replicates. PSMB3 bands are normalized to BACTIN bands and graphed relative to -RTA time 0 control.

Figure 9. RTA expression results in decreased peptide transport into the ER and decreased HLA in the ER. (a) Addition of 1μg/ml doxycycline (48h) induced RTA expression in iSLK cells. (b) Peptide transport assay. iSLK cells were treated with doxycline. 48hrs post treatment cells were harvested, semipermeablized and incubated with fluorescent peptides under the indicated conditions. (c) RTA expression results in decreased intracellular HLA staining. iSLK cells were treated +/- doxycycline (1μg/ml) to induce RTA expression. Cells were fixed, permeabilized and stained for HLA or CXCR5 as a control. Left histogram = unstained cells, right = stained cells.

Cells were analyzed using a Guava EasyCyte Flow cytometer. (d) Mean fluorescence intensity was analyzed for 3 replicate experiments using a ratio paired t test. *p=0.0243

1. Dittmer DP, Damania B. Kaposi sarcoma associated herpesvirus pathogenesis (KSHV)--an update. Curr Opin Virol. 2013;3: 238–44. doi:10.1016/j.coviro.2013.05.012
2. Dissinger NJ, Damania B. Recent advances in understanding Kaposi's sarcoma-associated herpesvirus. F1000Res. 2016;5: 740. doi:10.12688/f1000research.7612.1
3. Bower M, Nelson M, Young AM, Thirlwell C, Newsom-Davis T, Mandalia S, et al. Immune reconstitution inflammatory syndrome associated with Kaposi's sarcoma. Journal of Clinical Oncology. 2005;23: 5224–5228. doi:10.1200/JCO.2005.14.597
4. Uldrick TS, Wang V, Mahony DO, Aleman K, Wyvill KM, Marshall V, et al. An Interleukin-6 – Related Systemic Inflammatory Syndrome in Patients Co-Infected with Kaposi Sarcoma – Associated Herpesvirus and HIV but without Multicentric Castleman Disease. 2010;1868: 350–358. doi:10.1086/654798
5. Polizzotto MN, Uldrick TS, Hu D, Yarchoan R. Clinical manifestations of Kaposi sarcoma herpesvirus lytic activation: Multicentric Castleman disease (KSHV-MCD) and the KSHV inflammatory cytokine syndrome. Frontiers in Microbiology. 2012;3: 1–9. doi:10.3389/fmicb.2012.00073
6. Https://ntp.niehs.nih.gov/go/roc14 N (National TP. Report on Carcinogens, Fourteenth Edition. Research Triangle Park, NC: U.S.; 2016.
7. Cesarman E, Damania B, Krown SE, Martin J, Bower M, Whitby D. Kaposi sarcoma. Nature Reviews Disease Primers. 2019;5: 9. doi:10.1038/s41572-019-0060-9
8. Nakamura H, Lu M, Gwack Y, Souvlis J, Zeichner SL, Jung JU. Global Changes in Kaposis Sarcoma-Associated Virus Gene Expression Patterns following Expression of a Tetracycline-Inducible Rta Transactivator. Journal of Virology. 2003;77: 4205 LP – 4220. doi:10.1128/JVI.77.7.4205-4220.2003
9. Myoung J, Ganem D. Generation of a doxycycline-inducible KSHV producer cell line of endothelial origin: Maintenance of tight latency with efficient reactivation upon induction. Journal of Virological Methods. 2011;174: 12–21. doi:https://doi.org/10.1016/j.jviromet.2011.03.012
10. Yu Y, Hayward GS. The ubiquitin E3 ligase RAUL negatively regulates type i interferon through ubiquitination of the transcription factors IRF7 and IRF3. Immunity. 2010;33: 863–77. doi:10.1016/j.immuni.2010.11.027
11. Yu Y, Wang SE, Hayward GS. The KSHV immediate-early transcription factor RTA encodes ubiquitin E3 ligase activity that targets IRF7 for proteosome-mediated degradation. Immunity. 2005;22: 59–70. doi:10.1016/j.immuni.2004.11.011
12. Izumiya Y, Kobayashi K, Kim KY, Pochampalli M, Izumiya C, Shevchenko B, et al. Kaposi's Sarcoma-Associated Herpesvirus K-Rta Exhibits SUMO-Targeting Ubiquitin Ligase (STUbL) Like Activity and Is Essential for Viral Reactivation. PLoS Pathogens. 2013;9. doi:10.1371/journal.ppat.1003506
13. Campbell M, Izumiya Y. Post-translational modifications of Kaposi's sarcoma-associated herpesvirus regulatory proteins - SUMO and KSHV. Frontiers in Microbiology. 2012;3: 1–13. doi:10.3389/fmicb.2012.00031
14. Cai Q-L, Knight JS, Verma SC, Zald P, Robertson ES. EC5S ubiquitin complex is recruited by KSHV latent antigen LANA for degradation of the VHL and p53 tumor suppressors. PLoS Pathog. 2006;2: e116. doi:10.1371/journal.ppat.0020116
15. Zhao Q, Liang D, Sun R, Jia B, Xia T, Xiao H, et al. Kaposis Sarcoma-Associated Herpesvirus-Encoded Replication and Transcription Activator Impairs Innate Immunity via Ubiquitin-Mediated Degradation of Myeloid Differentiation Factor 88. Hutt-Fletcher LM, editor. Journal of Virology. 2015;89: 415 LP – 427. doi:10.1128/JVI.02591-14

16. Yang Z, Yan Z, Wood C. Kaposis Sarcoma-Associated Herpesvirus Transactivator RTA Promotes Degradation of the Repressors To Regulate Viral Lytic Replication. Journal of Virology. 2008;82: 3590 LP – 3603. doi:10.1128/JVI.02229-07
17. Gould F, Harrison SM, Hewitt EW, Whitehouse A. Kaposis Sarcoma-Associated Herpesvirus RTA Promotes Degradation of the Hey1 Repressor Protein through the Ubiquitin Proteasome Pathway. Journal of Virology. 2009;83: 6727 LP – 6738. doi:10.1128/JVI.00351-09
18. Combs LR, Spires LM, Alonso JD, Papp B, Toth Z. KSHV RTA Induces Degradation of the Host Transcription Repressor ID2 To Promote the Viral Lytic Cycle. Journal of Virology. 2022;96. doi:10.1128/jvi.00101-22
19. Ehrlich ES, Chmura JC, Smith JC, Kalu NN, Hayward GS. KSHV RTA abolishes NF B responsive gene expression during lytic reactivation by targeting vFLIP for degradation via the proteasome. PLoS ONE. 2014;9. doi:10.1371/journal.pone.0091359
20. Chmura JC, Herold K, Ruffin A, Atuobi T, Fabiyi Y, Mitchell AE, et al. The Itch ubiquitin ligase is required for KSHV RTA induced vFLIP degradation. Virology. 2017;501. doi:10.1016/j.virol.2016.11.016
21. Ong SE, Mann M. A practical recipe for stable isotope labeling by amino acids in cell culture (SILAC). Nature Protocols. 2007;1: 2650–2660. doi:10.1038/nprot.2006.427
22. Cox J, Mann M. MaxQuant enables high peptide identification rates, individualized p.p.b.-range mass accuracies and proteome-wide protein quantification. Nature Biotechnology. 2008;26: 1367–1372. doi:10.1038/NBT.1511
23. Cox J, Neuhauser N, Michalski A, Scheltema RA, Olsen J v., Mann M. Andromeda: A peptide search engine integrated into the MaxQuant environment. Journal of Proteome Research. 2011;10: 1794–1805. doi:10.1021/pr101065j
24. Tyanova S, Temu T, Sinitcyn P, Carlson A, Hein MY, Geiger T, et al. The Perseus computational platform for comprehensive analysis of (prote)omics data. Nature Methods. 2016. doi:10.1038/nmeth.3901
25. DeCotiis JL, Ortiz NC, Vega BA, Lukac DM. An easily transfectable cell line that produces an infectious reporter virus for routine and robust quantitation of Kaposi's sarcoma-associated herpesvirus reactivation. Journal of Virological Methods. 2017;247: 99–106. doi:10.1016/j.jviromet.2017.04.019
26. Coscoy L, Ganem D. Kaposi's sarcoma-associated herpesvirus encodes two proteins that block cell surface display of MHC class I chains by enhancing their endocytosis. Proceedings of the National Academy of Sciences. 2002;97: 8051–8056. doi:10.1073/pnas.140129797
27. Parkinson MDJ, Piper SC, Bright NA, Evans JL, Boname JM, Bowers K, et al. A non-canonical ESCRT pathway, including histidine domain phosphotyrosine phosphatase (HD-PTP), is used for down-regulation of virally ubiquitinated MHC class I. Biochemical Journal. 2015;471: 79–88. doi:10.1042/BJ20150336
28. Goto E, Yamanaka Y, Ishikawa A, Aoki-Kawasumi M, Mito-Yoshida M, Ohmura-Hoshino M, et al. Contribution of Lysine 11-linked Ubiquitination to MIR2-mediated Major Histocompatibility Complex Class I Internalization. Journal of Biological Chemistry . 2010;285: 35311–35319. doi:10.1074/jbc.M110.112763
29. Pardieu C, Vigan R, Wilson SJ, Calvi A, Zang T, Bieniasz P, et al. The RING-CH Ligase K5 Antagonizes Restriction of KSHV and HIV-1 Particle Release by Mediating Ubiquitin-Dependent Endosomal Degradation of Tetherin. PLoS Pathogens. 2010;6: e1000843. doi:10.1371/journal.ppat.1000843
30. Campadelli-Fiume G, Collins-McMillen D, Gianni T, Yurochko AD. Integrins as Herpesvirus Receptors and Mediators of the Host Signalosome. Annual Review of Virology. 2016;3: 215–236. doi:10.1146/annurev-virology-110615-035618

31. Feire AL, Koss H, Compton T. Cellular integrins function as entry receptors for human cytomegalovirus via a highly conserved disintegrin-like domain. 2004. Available: www.pnas.orgcgidoi10.1073pnas.0406821101
32. Szklarczyk D, Gable AL, Lyon D, Junge A, Wyder S, Huerta-Cepas J, et al. STRING v11: protein–protein association networks with increased coverage, supporting functional discovery in genome-wide experimental datasets. Nucleic Acids Research. 2018;47: D607–D613. doi:10.1093/nar/gky1131
33. Huang DW, Sherman BT, Lempicki RA. Bioinformatics enrichment tools: paths toward the comprehensive functional analysis of large gene lists. Nucleic Acids Research. 2008;37: 1–13. doi:10.1093/nar/gkn923
34. Huang J, Wang Y, Guo Y, Sun S. Down-regulated microRNA-152 induces aberrant DNA methylation in hepatitis B virus-related hepatocellular carcinoma by targeting DNA methyltransferase 1. Hepatology. 2010;52: 60–70. doi:10.1002/hep.23660
35. Cirone M. EBV and KSHV Infection Dysregulates Autophagy to Optimize Viral Replication, Prevent Immune Recognition and Promote Tumorigenesis. Viruses. 2018;10: 1–10. doi:10.3390/v10110599
36. Santarelli R, Granato M, Pentassuglia G, Lacconi V, Gilardini Montani MS, Gonnella R, et al. KSHV reduces autophagy in THP-1 cells and in differentiating monocytes by decreasing CAST/calpastatin and ATG5 expression. Autophagy. 2016;12: 2311–2325. doi:10.1080/15548627.2016.1235122
37. Ishido S, Wang C, Lee B-S, Cohen GB, Jung JU. Downregulation of Major Histocompatibility Complex Class I Molecules by Kaposis Sarcoma-Associated Herpesvirus K3 and K5 Proteins. Journal of Virology. 2000;74: 5300 LP – 5309. doi:10.1128/JVI.74.11.5300-5309.2000
38. Ressing Kremmer ME, Rickinson AB, Wiertz EJHJ, Garstka MA, Hislop AD, Horst ED, et al. Antigen Presentation Impairment of HLA Class I-Restricted Associated with Antigen Processing Results in Protein BNLF2a to the Transporter Specific Targeting of the EBV Lytic Phase. 2009. doi:10.4049/jimmunol.0803218
39. Bennett EM, Bennink JR, Yewdell JW, Brodsky FM. Cutting edge: adenovirus E19 has two mechanisms for affecting class I MHC expression. J Immunol. 1999;162.
40. Ahn K, Gruhler A. The ER-Luminal Domain of the HCMV Glycoprotein US6 Inhibits Peptide Translocation by TAP. Immunity. 1997.
41. Ahn K, Meyer TH, Uebel S, Sempé P, Djaballah H, Yang Y, et al. Molecular mechanism and species specificity of TAP inhibition by herpes simplex virus protein ICP47. EMBO Journal. 1996;15: 3247–3255. doi:10.1002/j.1460-2075.1996.tb00689.x
42. Fischbach H, Döring M, Nikles D, Lehnert E, Baldauf C, Kalinke U, et al. ARTICLE Ultrasensitive quantification of TAP-dependent antigen compartmentalization in scarce primary immune cell subsets. 2015. doi:10.1038/ncomms7199
43. Hughes EA, Hammond C, Cresswell P, Amos DB. Misfolded major histocompatibility complex class I heavy chains are translocated into the cytoplasm and degraded by the proteasome. 1997. Available: www.pnas.org.
44. Burr ML, van den Boomen DJH, Bye H, Antrobus R, Wiertz EJ, Lehner PJ. MHC class I molecules are preferentially ubiquitinated on endoplasmic reticulum luminal residues during HRD1 ubiquitin E3 ligase-mediated dislocation. Proc Natl Acad Sci U S A. 2013;110: 14290–14295. doi:10.1073/pnas.1303380110
45. Lubyova B, Kellum MJ, Frisancho AJ, Pitha PM. Kaposi's Sarcoma-associated Herpesvirus-encoded vIRF-3 Stimulates the Transcriptional Activity of Cellular IRF-3 and IRF-7. Journal of Biological Chemistry . 2004;279: 7643–7654. doi:10.1074/jbc.M309485200
46. Zhao Q, Liang D, Sun R, Jia B, Xia T, Xiao H, et al. Kaposi's Sarcoma-Associated Herpesvirus-Encoded Replication and Transcription Activator Impairs Innate Immunity via

Ubiquitin-Mediated Degradation of Myeloid Differentiation Factor 88. Journal of Virology. 2015;89: 415–427. doi:10.1128/jvi.02591-14
47. Han C, Zhang D, Gui C, Huang L, Chang S, Dong L, et al. KSHV RTA antagonizes SMC5/6 complex-induced viral chromatin compaction by hijacking the ubiquitin-proteasome system. 2022. doi:10.1371/journal.ppat.1010744
48. Jha HC, Upadhyay SK, AJ MP, Lu J, Cai Q, Saha A, et al. H2AX Phosphorylation Is Important for LANA-Mediated Kaposi's Sarcoma-Associated Herpesvirus Episome Persistence. Journal of Virology. 2013;87: 5255–5269. doi:10.1128/jvi.03575-12
49. Singh VV, Dutta D, Ansari MA, Dutta S, Chandran B. Kaposi's Sarcoma-Associated Herpesvirus Induces the ATM and H2AX DNA Damage Response Early during De Novo Infection of Primary Endothelial Cells, Which Play Roles in Latency Establishment . Journal of Virology. 2014;88: 2821–2834. doi:10.1128/jvi.03126-13
50. Pan MR, Peng G, Hungs WC, Lin SY. Monoubiquitination of H2AX protein regulates DNA damage response signaling. Journal of Biological Chemistry. 2011;286: 28599–28607. doi:10.1074/jbc.M111.256297
51. Hollingworth R, Horniblow RD, Forrest C, Stewart GS, Grand RJ. Localization of Double-Strand Break Repair Proteins to Viral Replication Compartments following Lytic Reactivation of Kaposi's Sarcoma-Associated Herpesvirus. 2017. doi:10.1128/JVI.00930-17
52. Gantt S, Carlsson J, Ikoma M, Gachelet E, Gray M, Geballe AP, et al. The HIV protease inhibitor nelfinavir inhibits Kaposi's sarcoma-associated herpesvirus replication in vitro. Antimicrobial Agents and Chemotherapy. 2011;55: 2696–2703. doi:10.1128/AAC.01295-10
53. The EMBO Journal - 2001 - Hewitt - The human cytomegalovirus gene product US6 inhibits ATP binding by TAP.
54. Hewitt EW, Lehner PJ. The ABC-transporter signature motif is required for peptide translocation but not peptide binding by TAP.

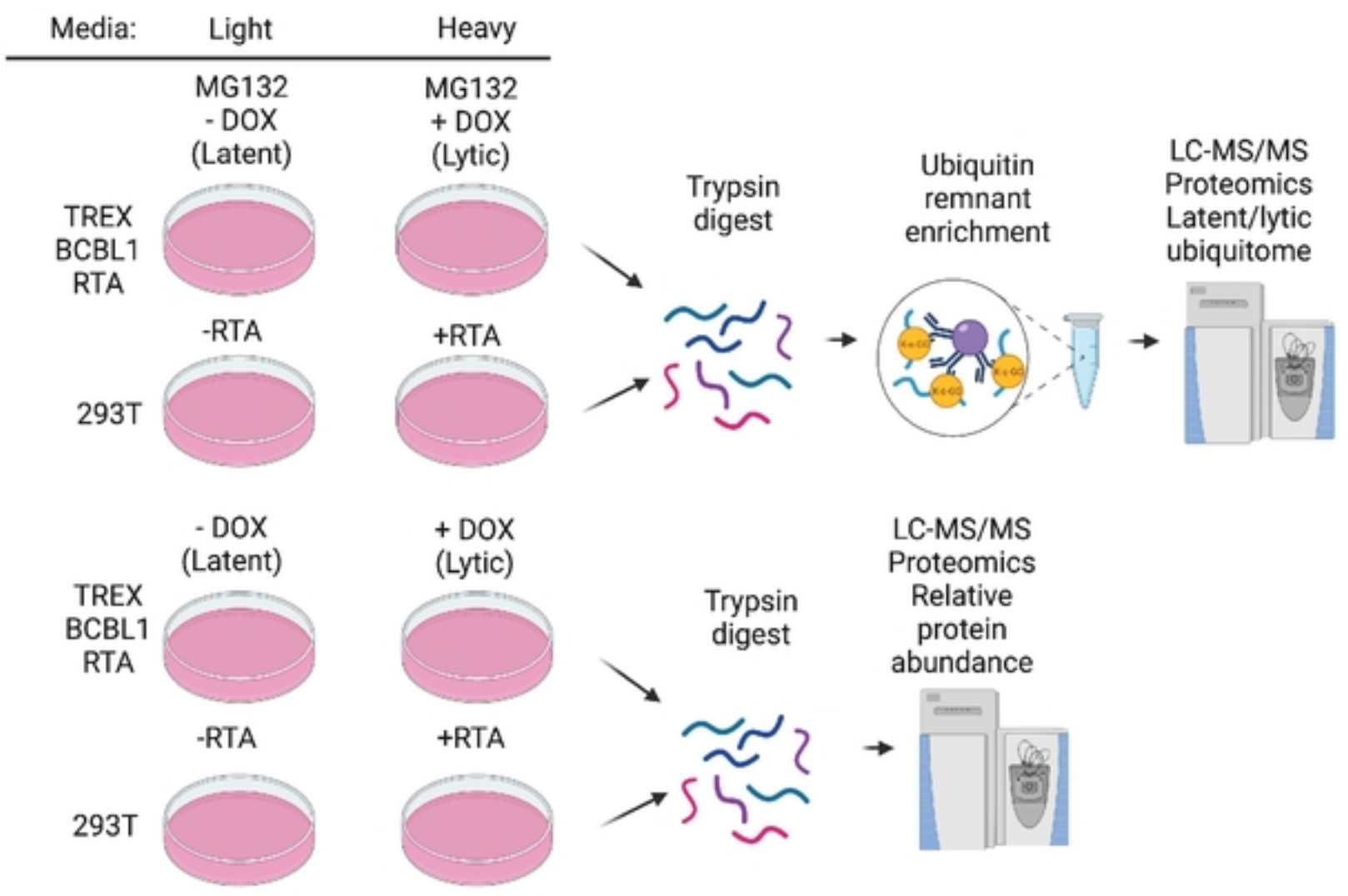
Media:
Light
Heavy
MG132
- DOX
(Latent)
MG132
+ DOX
(Lytic)
TREX
BCBL1
RTA
-RTA
+RTA
293T
Trypsin
digest
Ubiquitin
remnant
enrichment
LC-MS/MS
Proteomics
Latent/lytic
ubiquitome
- DOX
(Latent)
+ DOX
(Lytic)
TREX
BCBL1
RTA
-RTA
+RTA
293T
Trypsin
digest
LC-MS/MS
Proteomics
Relative
protein
abundance

Figure 1

A

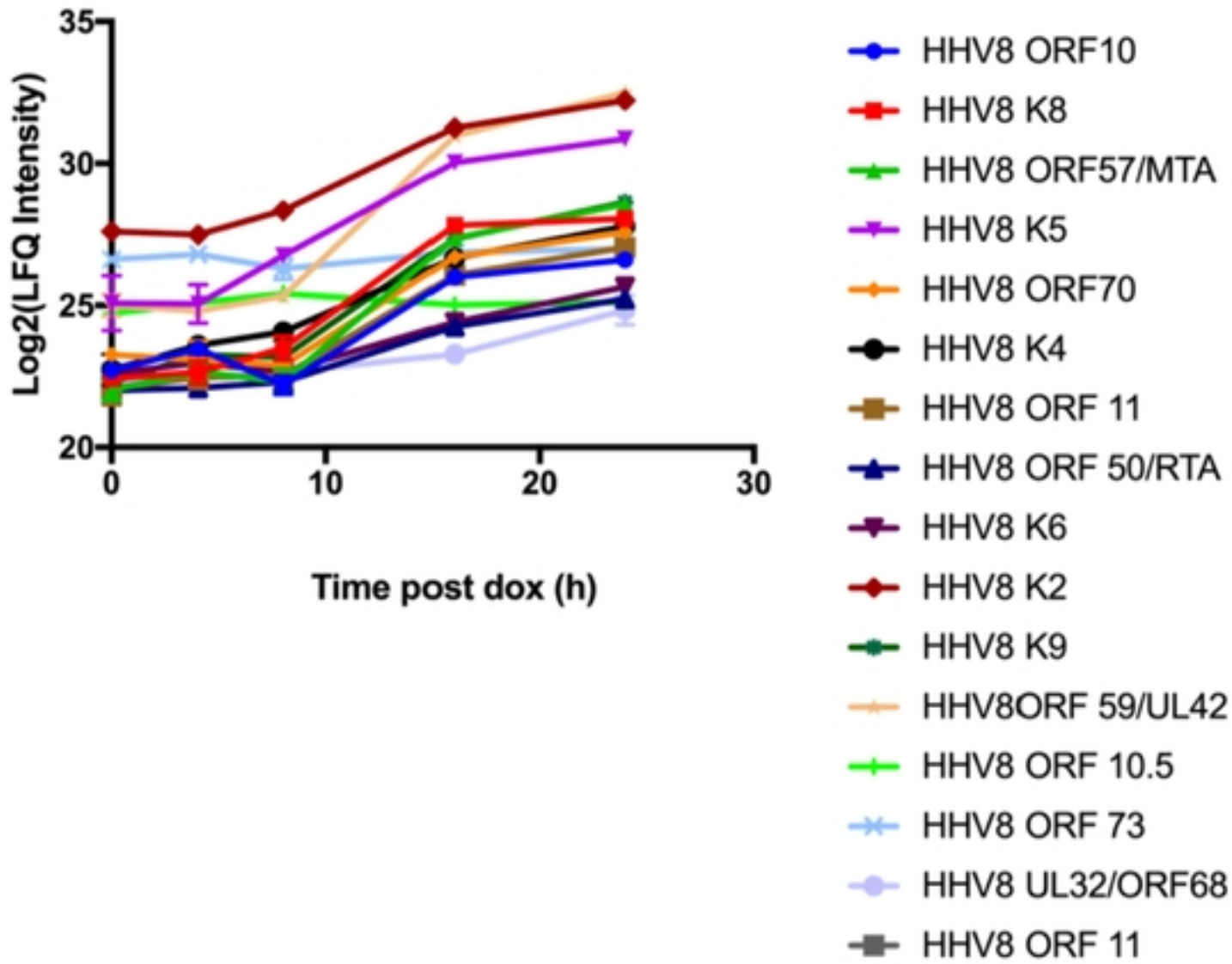

B

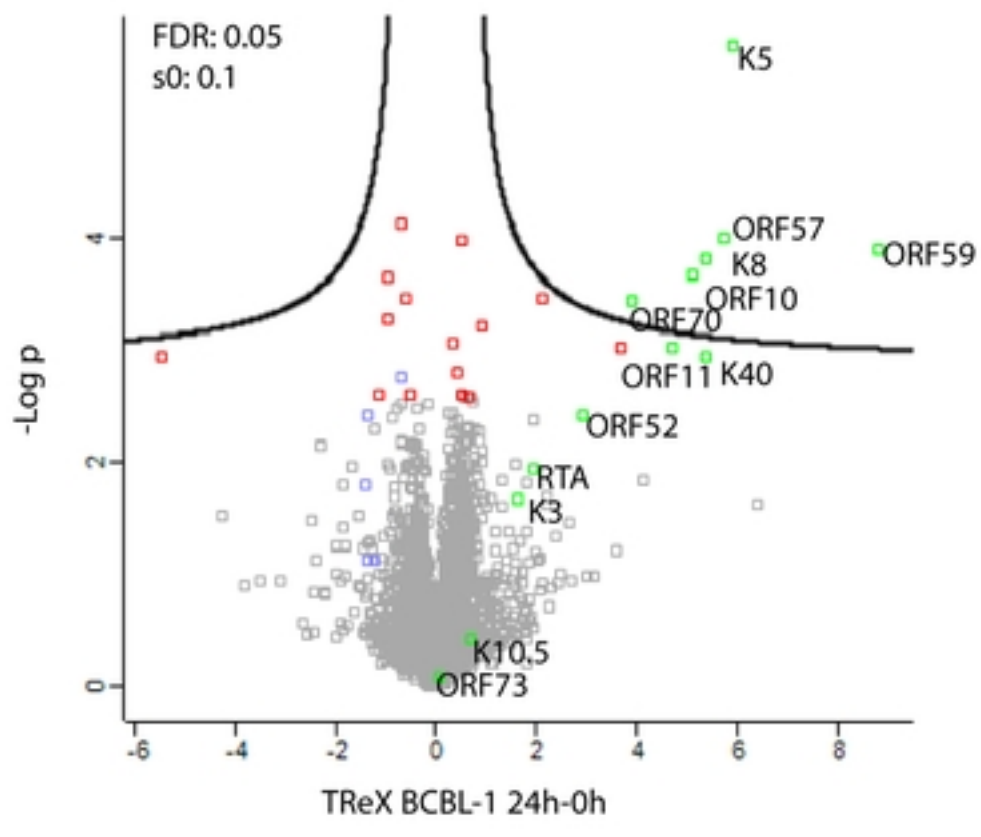

C

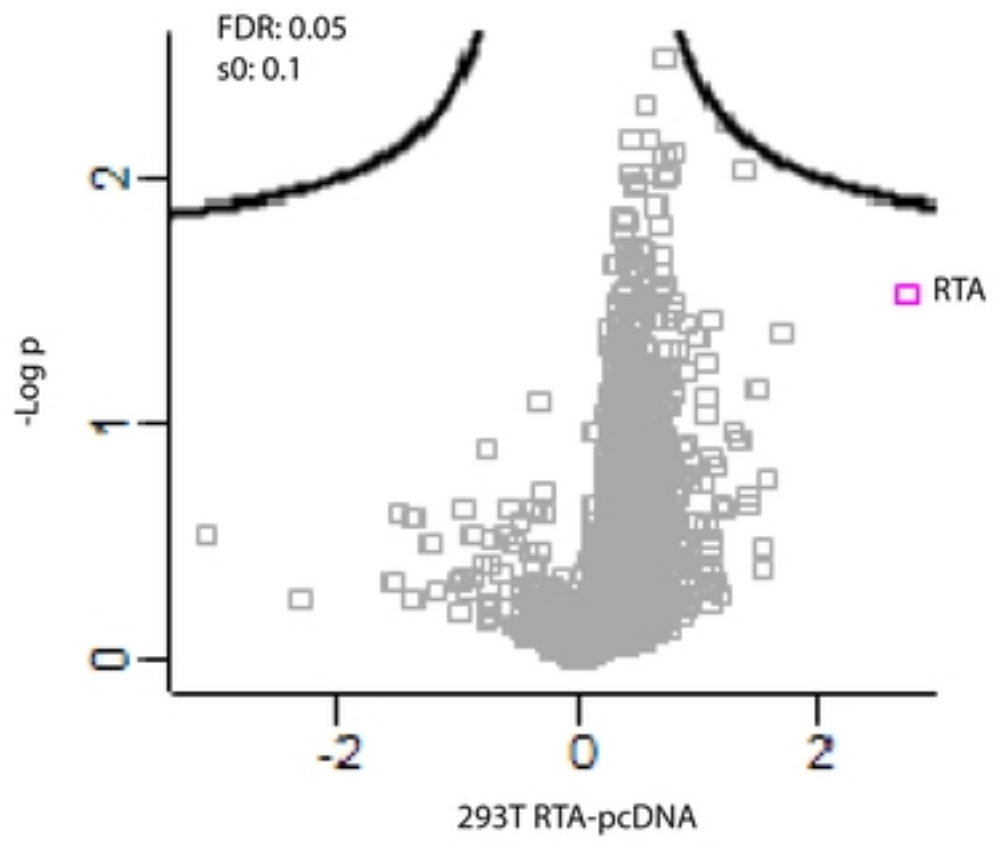

D

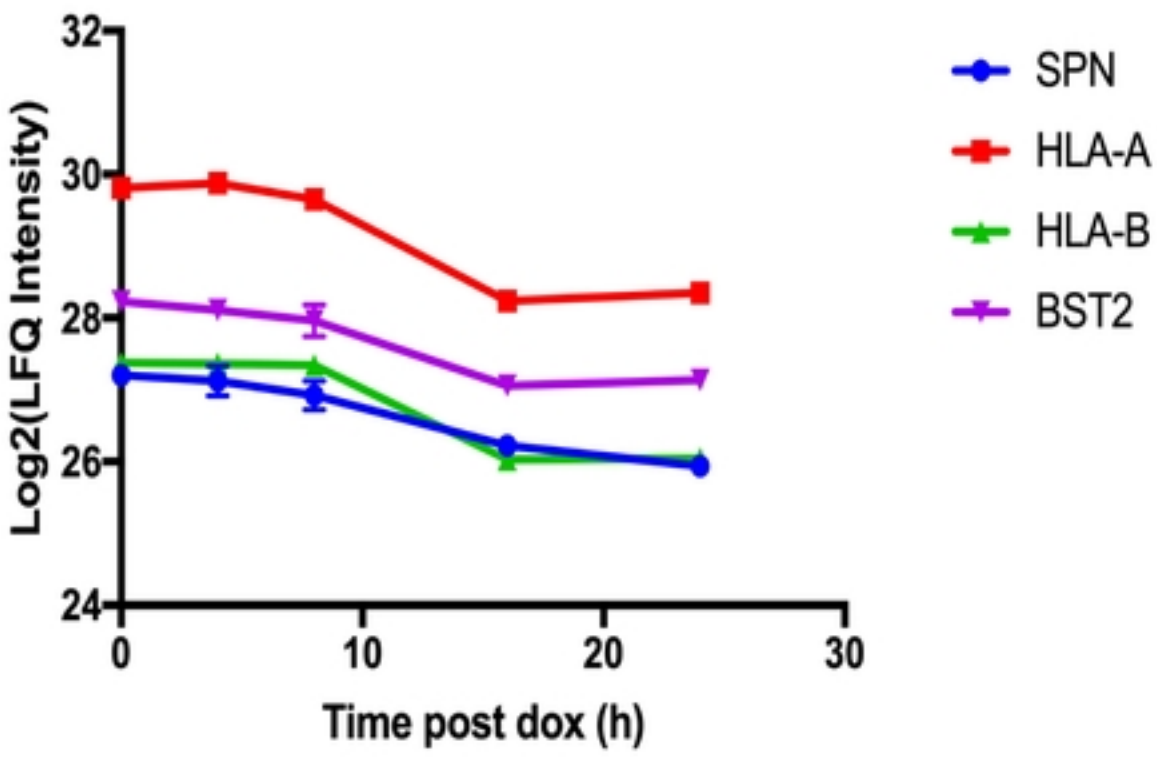

E

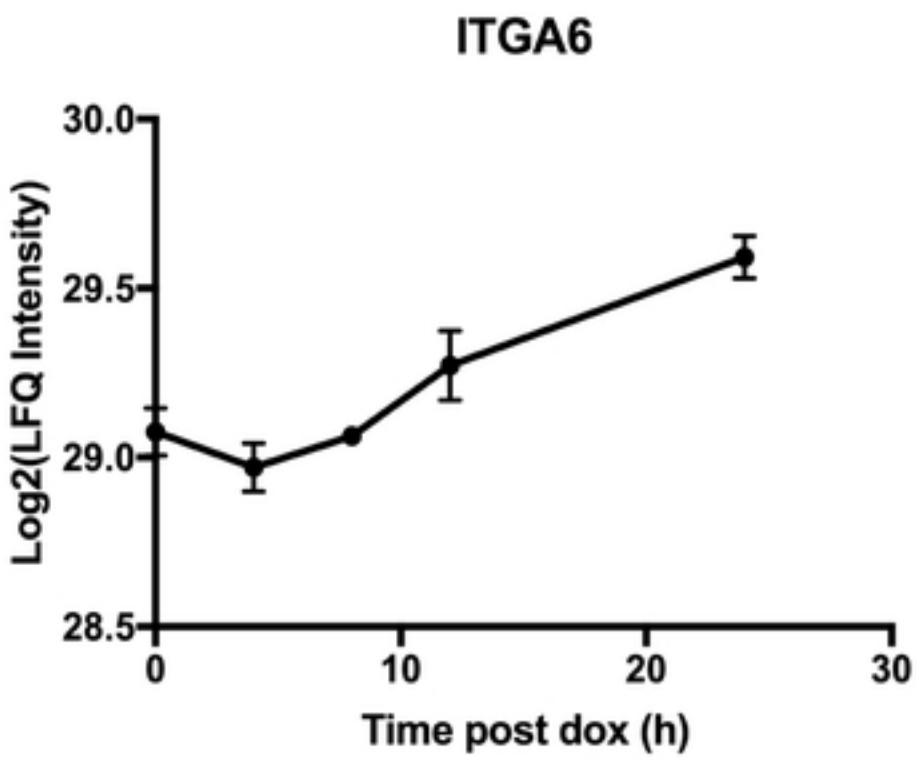

Figure 2

A

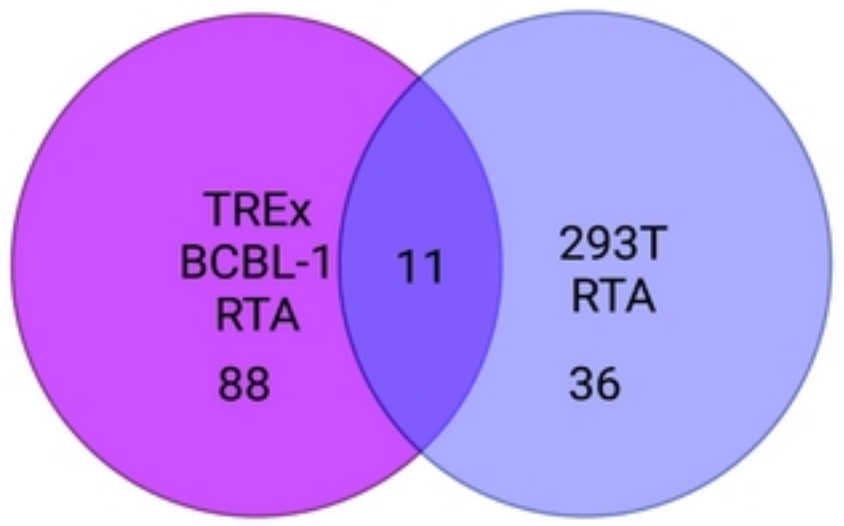

B

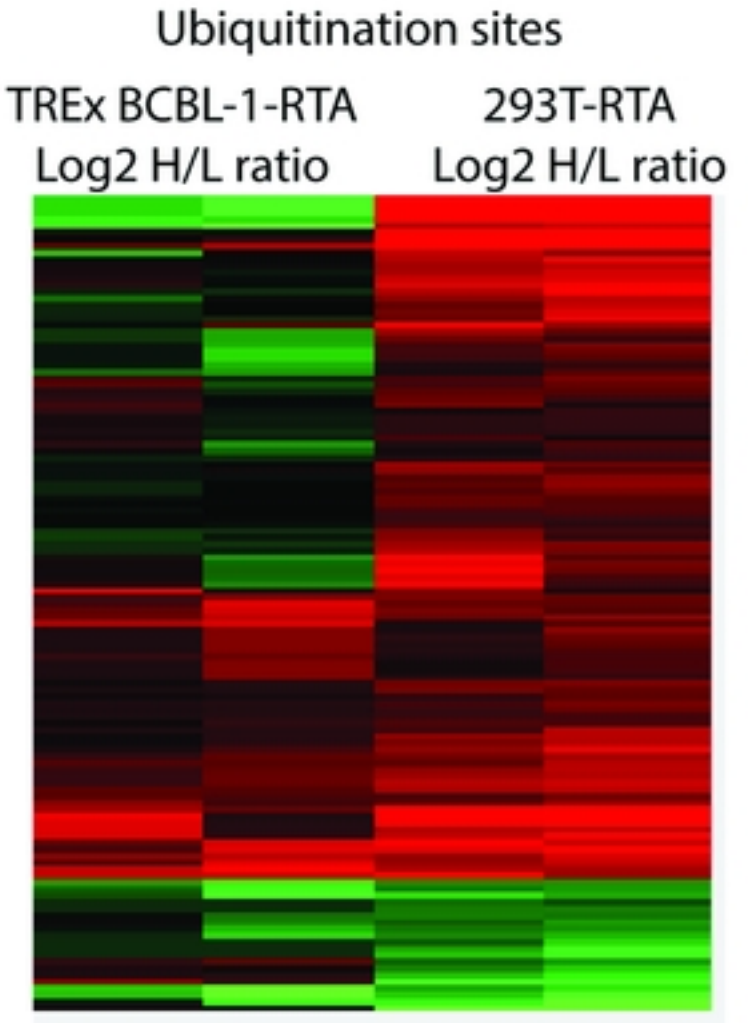

C

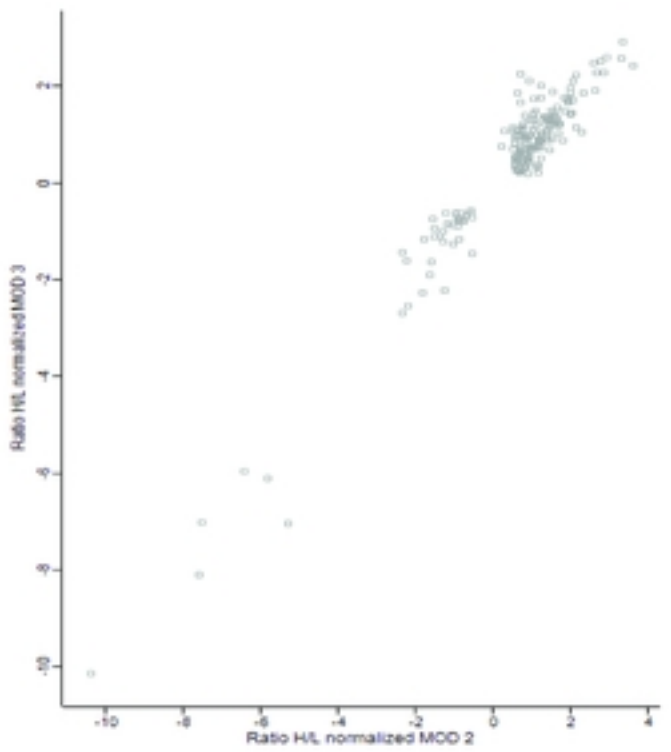

D

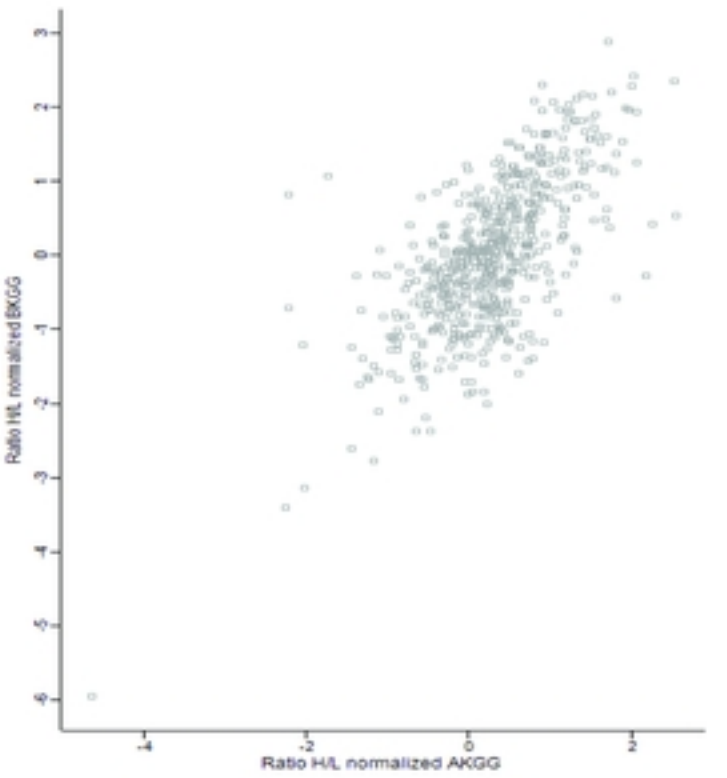

E

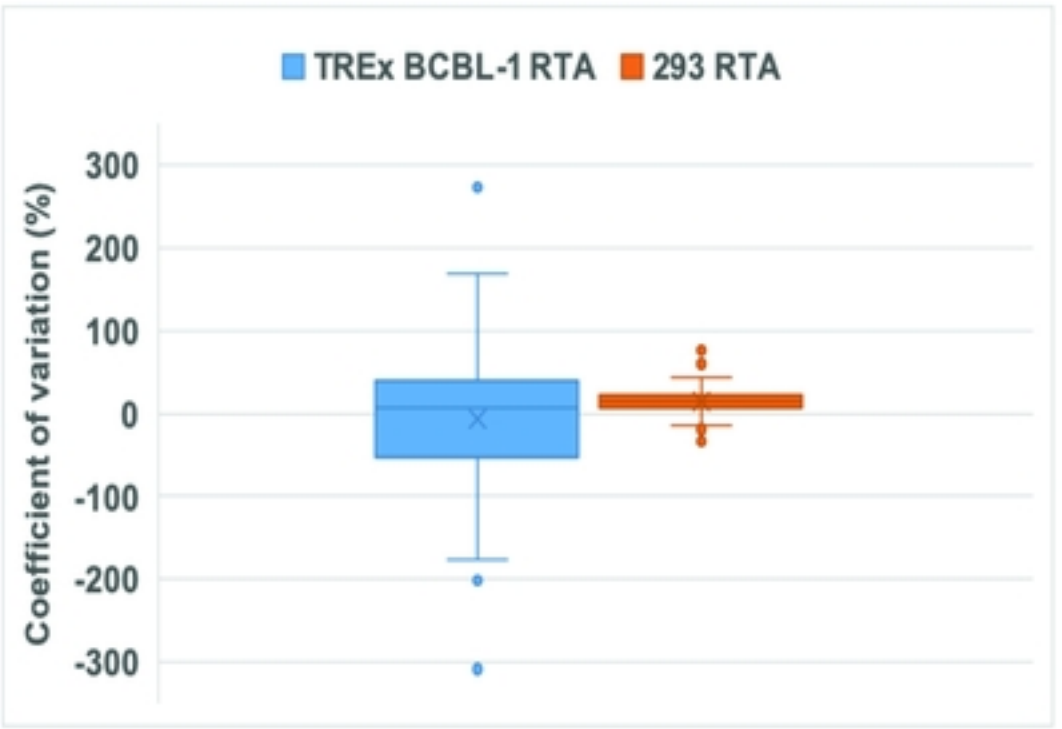

F

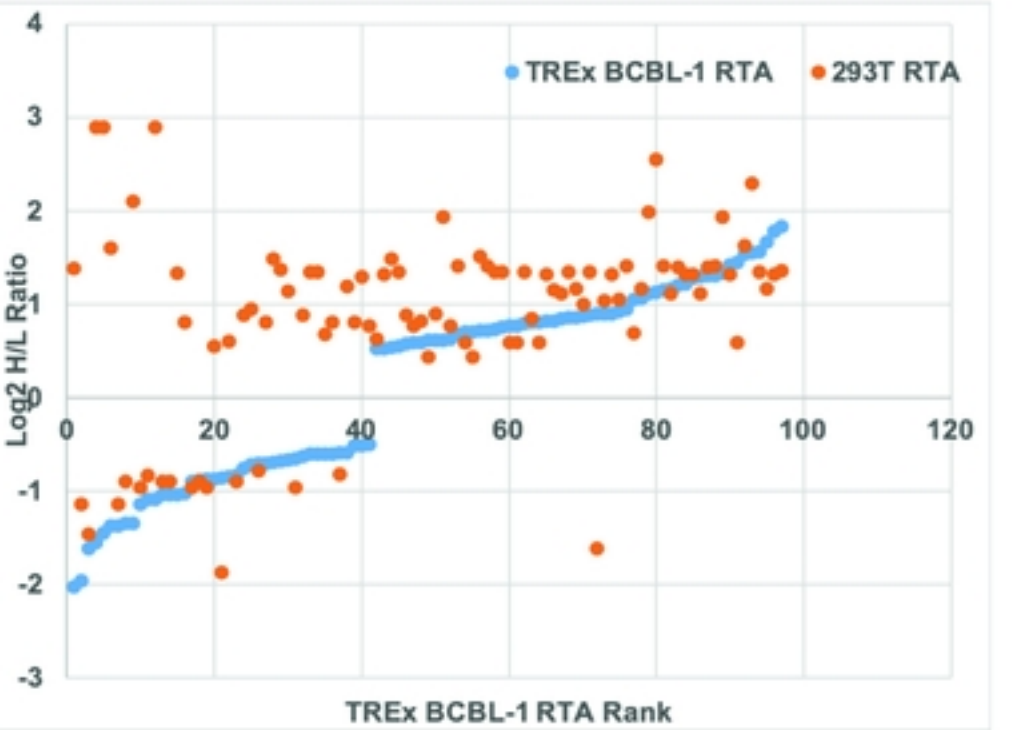

Figure 3

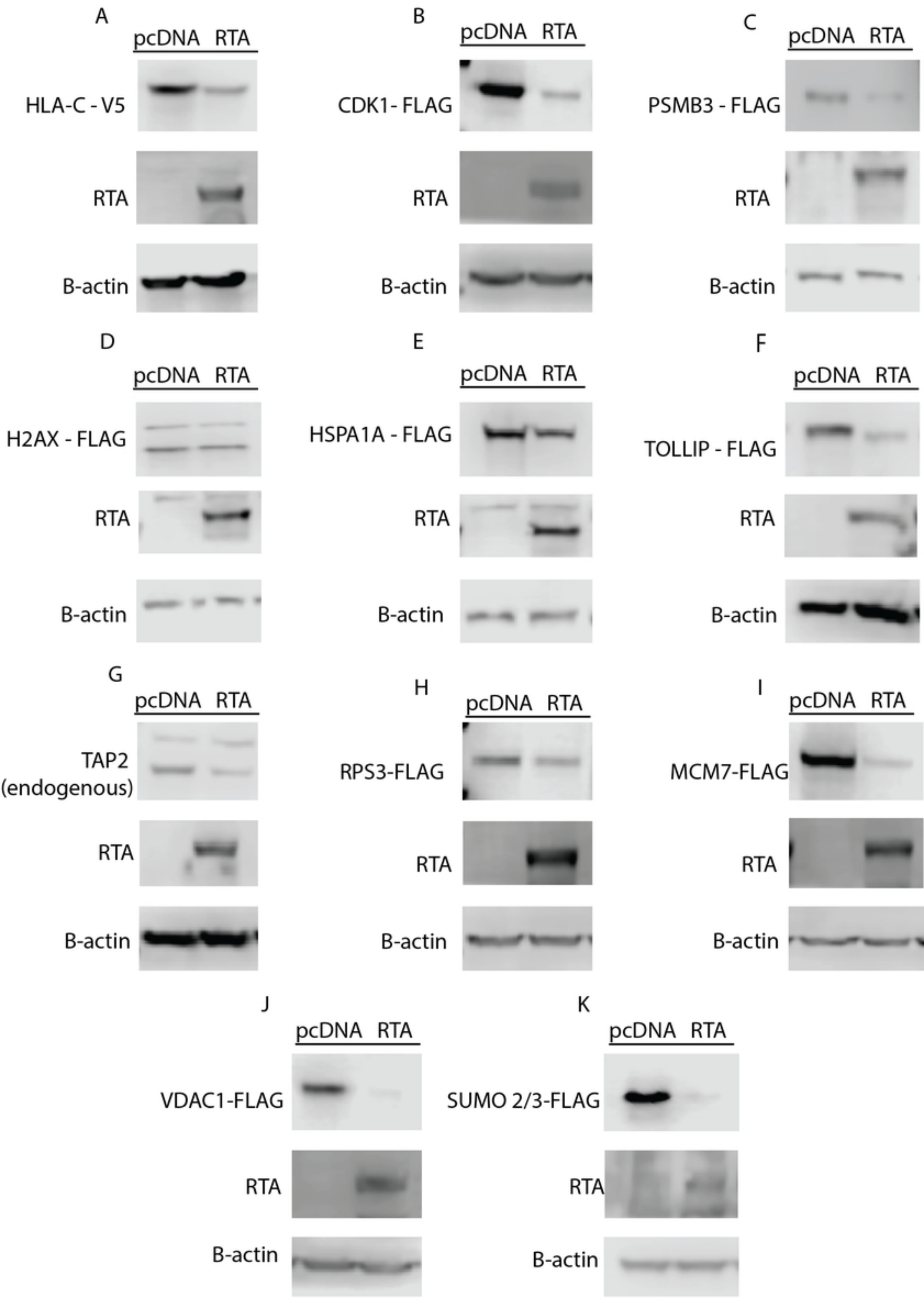
A
pcDNA RTA
HLA-C - V5
RTA
B-actin
B
pcDNA RTA
CDK1- FLAG
RTA
B-actin
C
pcDNA RTA
PSMB3 - FLAG
RTA
B-actin
D
pcDNA RTA
H2AX - FLAG
RTA
B-actin
E
pcDNA RTA
HSPA1A - FLAG
RTA
B-actin
F
pcDNA RTA
TOLLIP - FLAG
RTA
B-actin
G
pcDNA RTA
TAP2
(endogenous)
RTA
B-actin
H
pcDNA RTA
RPS3-FLAG
RTA
B-actin
I
pcDNA RTA
MCM7-FLAG
RTA
B-actin
J
pcDNA RTA
VDAC1-FLAG
RTA
B-actin
K
pcDNA RTA
SUMO 2/3-FLAG
RTA
B-actin

Figure 5

A

Uniprot ID	GENE NAME	BCBL-1 H/L A	BCBL1 H/L B	293T RTA H/L 1	293T RTA H/L 2
P61956	SUMO3;SUMO2	2.56	0.53	2.41	2.19
P61956	SUMO2	2.26	0.42	2.02	1.86

B

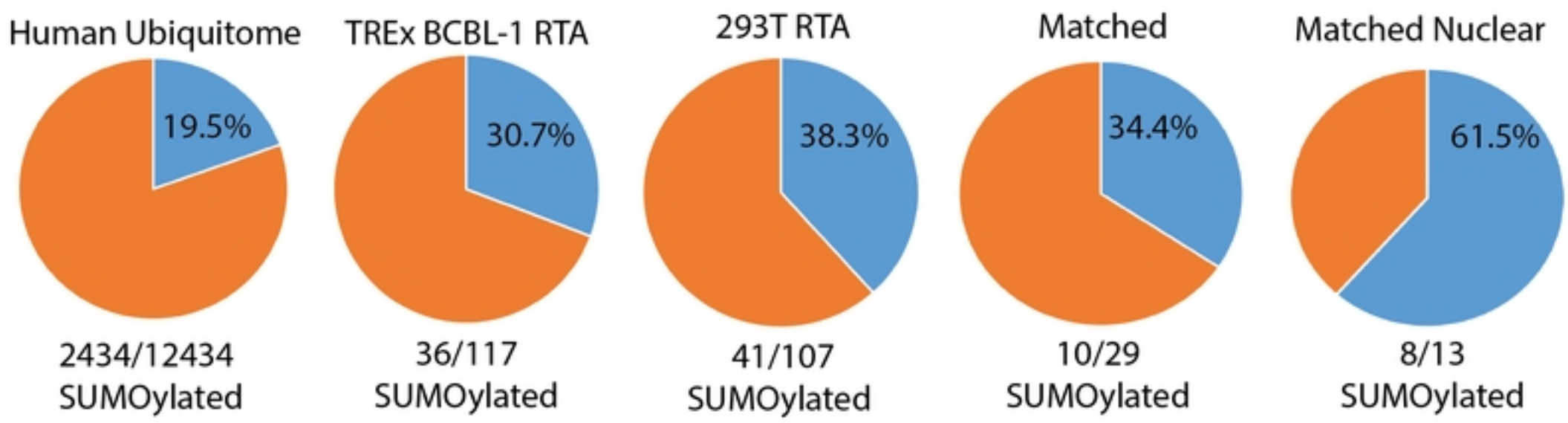

C

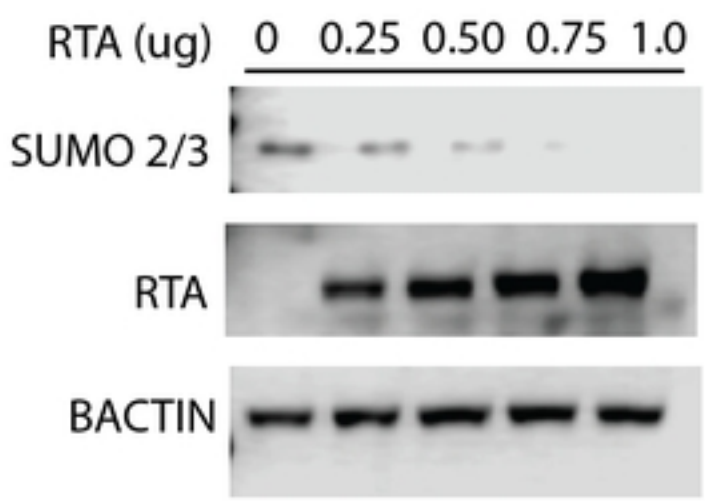

D

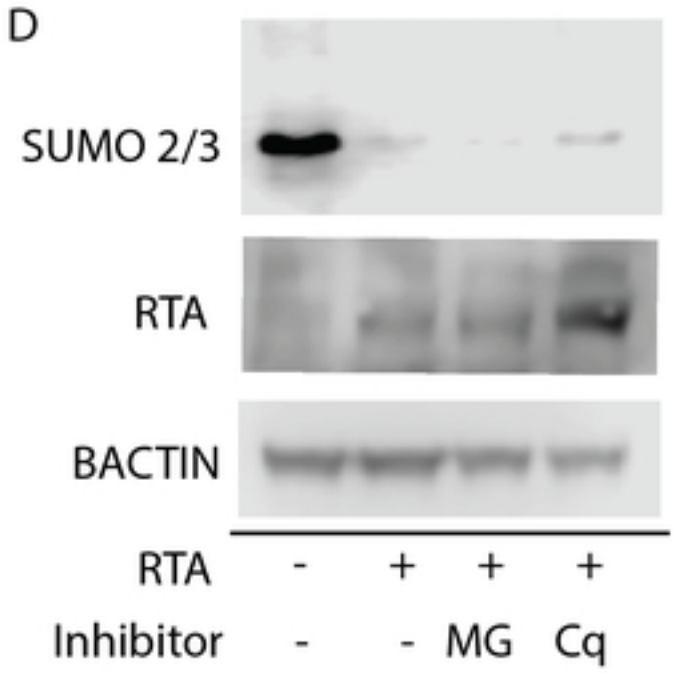

E

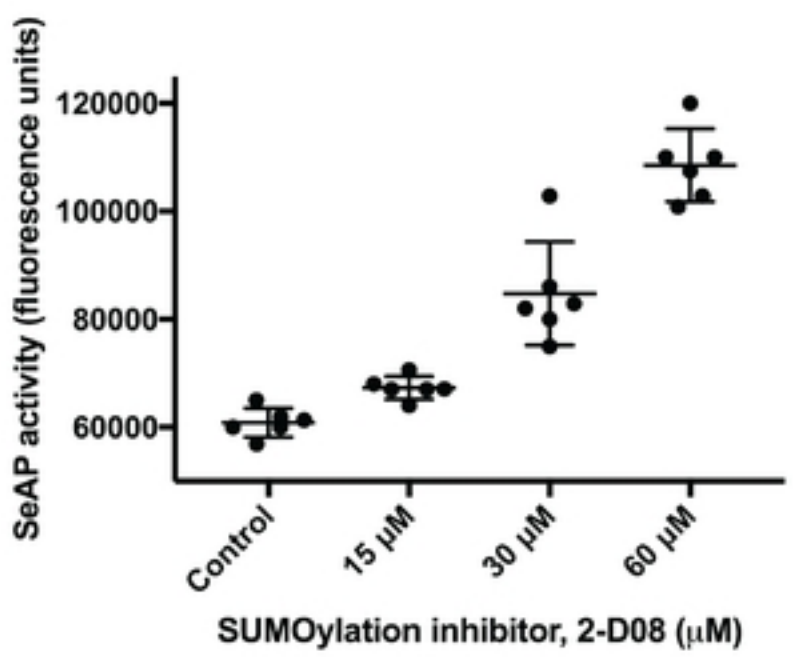

F

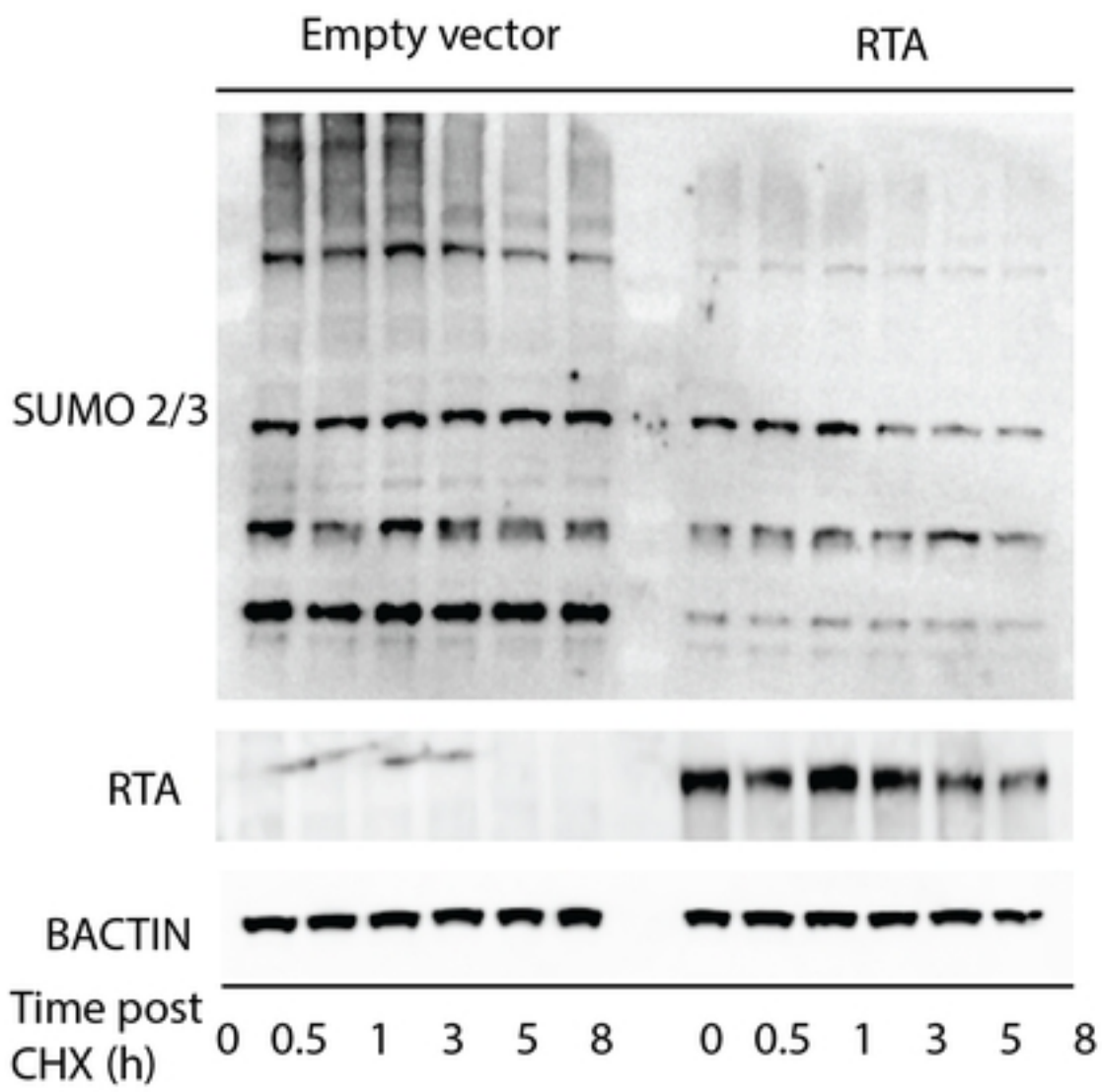

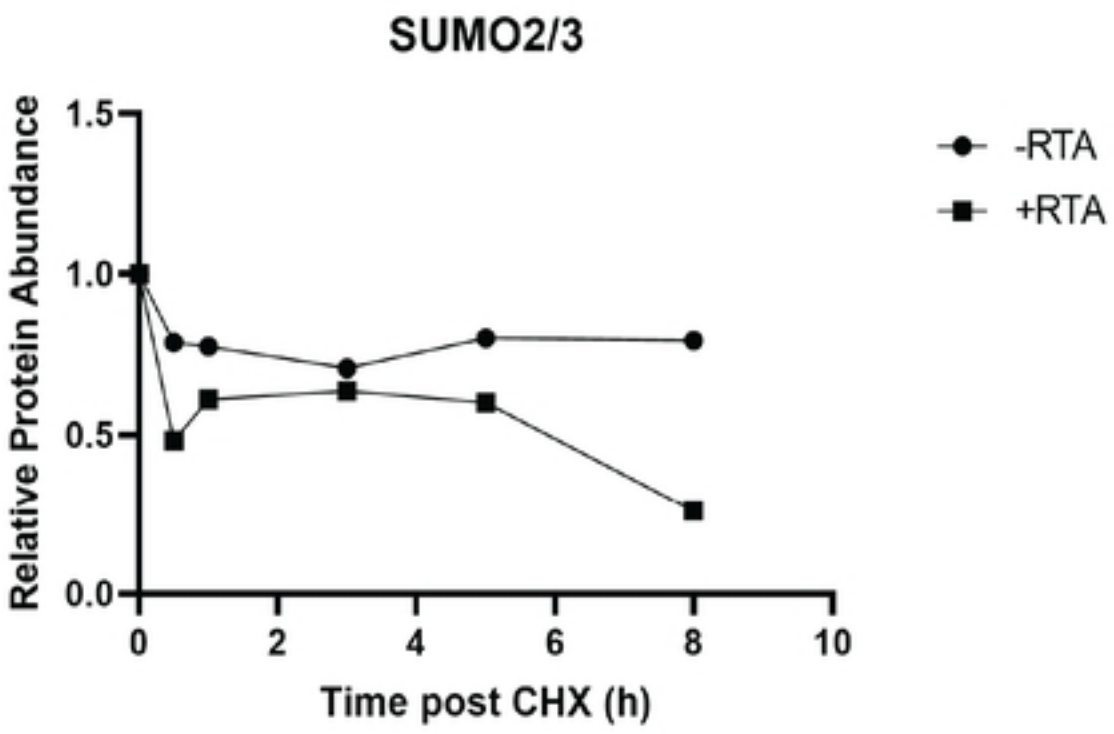

Figure 6

A

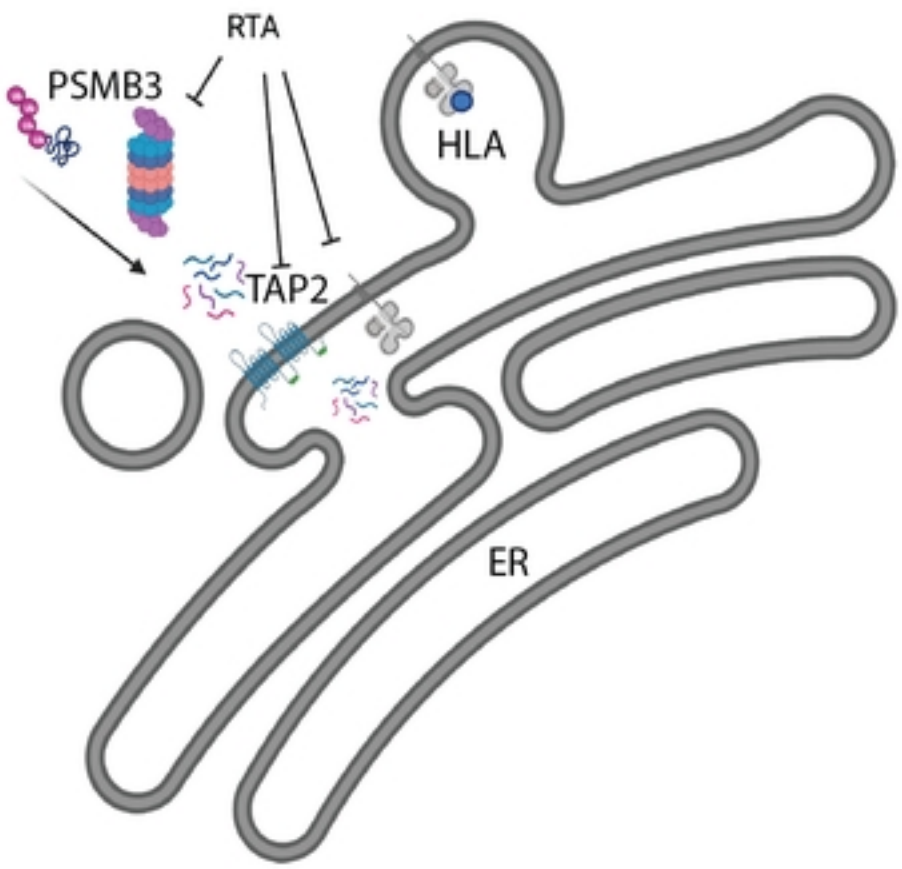
RTA
PSMB3
HLA
TAP2
ER

B

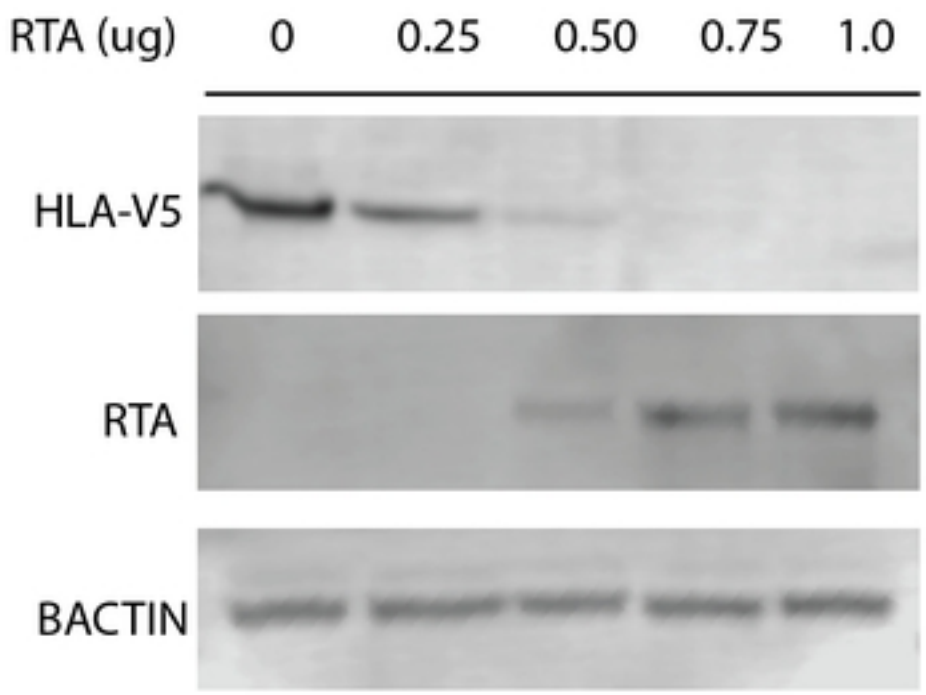
RTA (ug)
0
0.25
0.50
0.75
1.0
HLA-V5
RTA
BACTIN

C

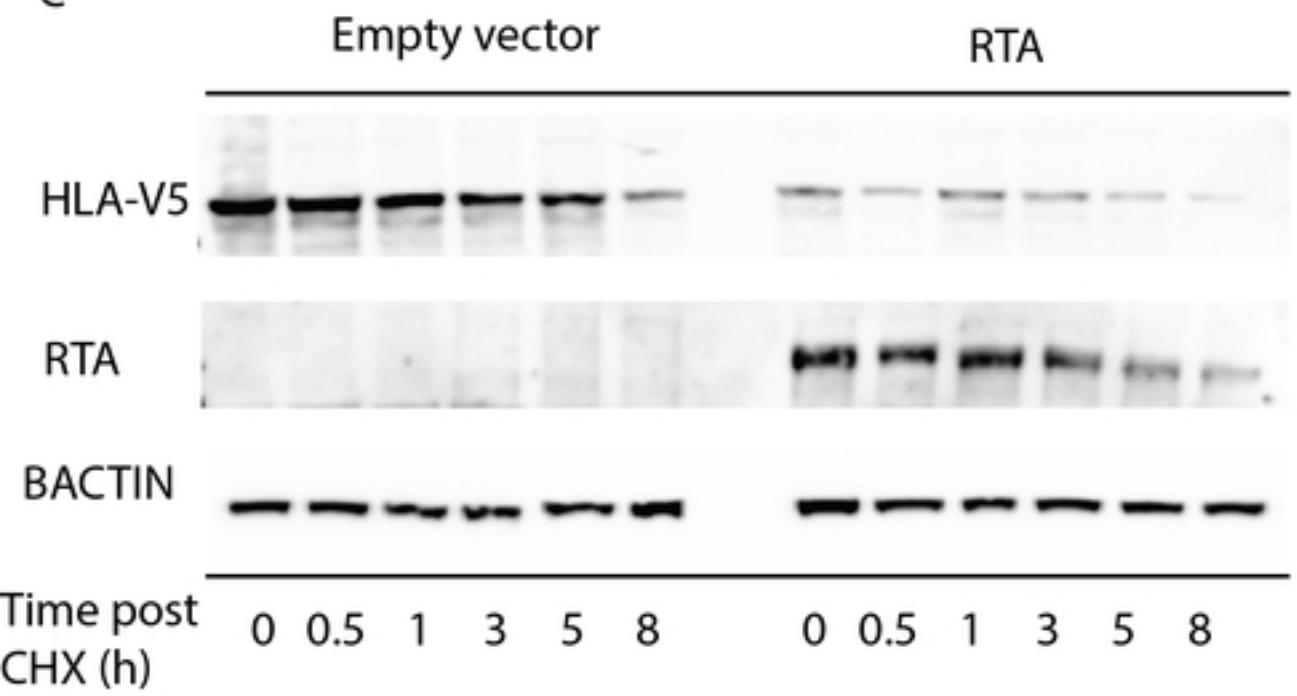
Empty vector
RTA
HLA-V5
RTA
BACTIN
Time post CHX (h)
0 0.5 1 3 5 8
0 0.5 1 3 5 8

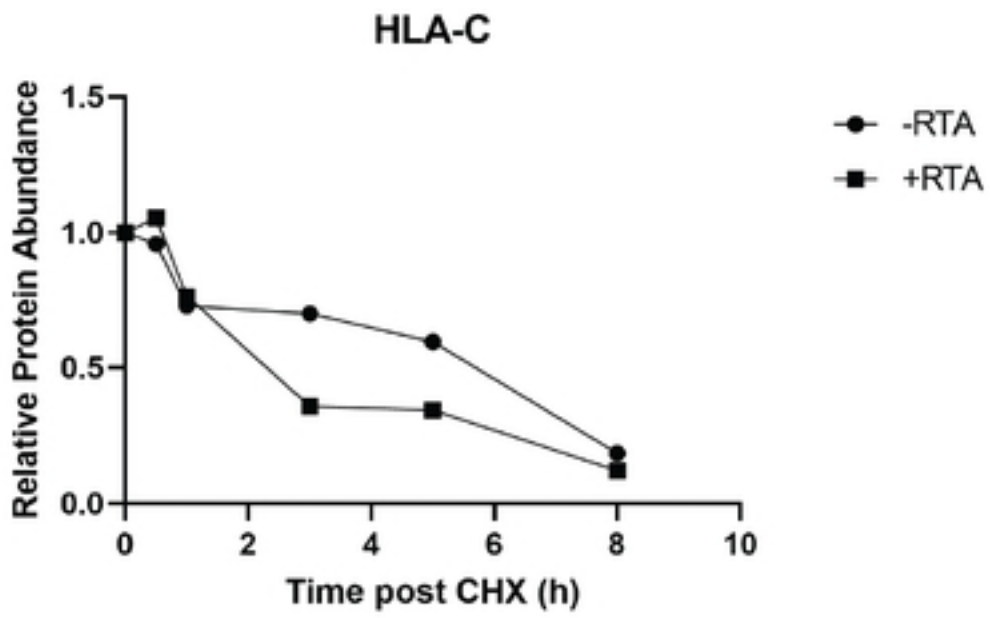
HLA-C
-RTA
+RTA
Relative Protein Abundance
1.5
1.0
0.5
0.0
0
2
4
6
8
10
Time post CHX (h)

Figure 7

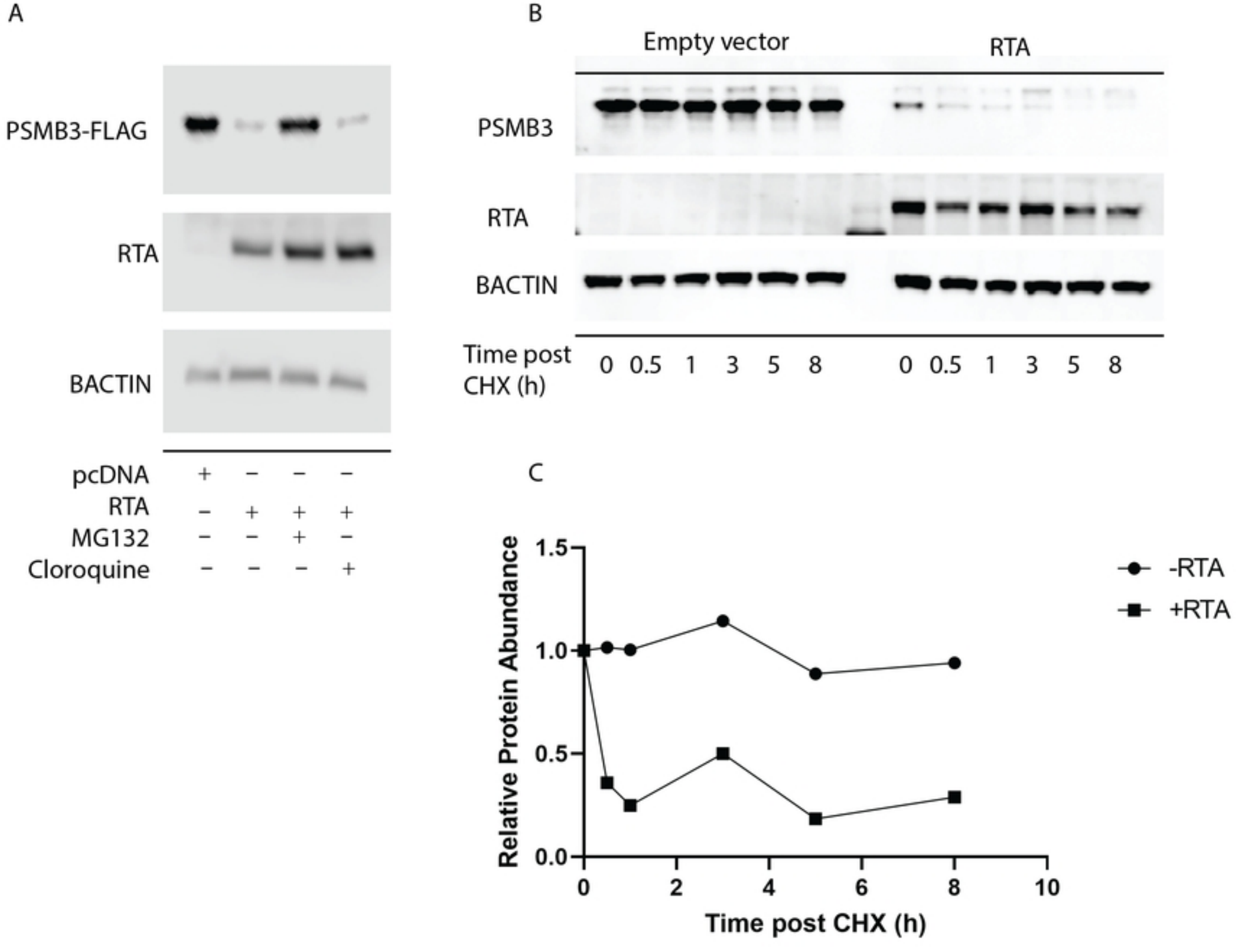
A
PSMB3-FLAG
RTA
BACTIN
pcDNA + − − −
RTA − + + +
MG132 − − + −
Cloroquine − − − +
B
Empty vector
RTA
PSMB3
RTA
BACTIN
Time post CHX (h)
0 0.5 1 3 5 8
0 0.5 1 3 5 8
C
Relative Protein Abundance
1.5
1.0
0.5
0.0
0
2
4
6
8
10
Time post CHX (h)
-RTA
+RTA

Figure 8

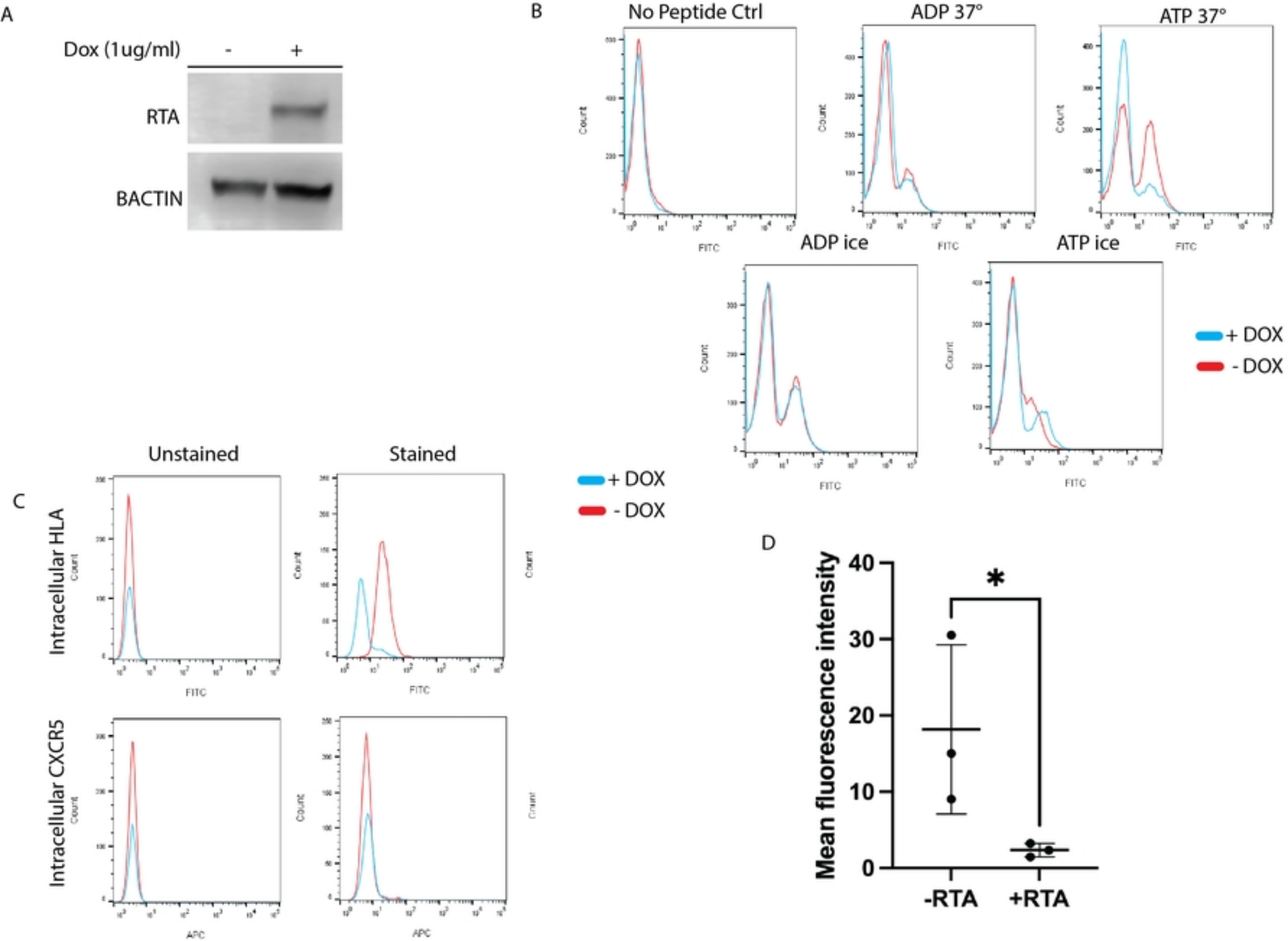
A
Dox (1ug/ml)
-
+
RTA
BACTIN
B
No Peptide Ctrl
ADP 37°
ATP 37°
ADP ice
ATP ice
Count
FITC
+ DOX
- DOX
C
Unstained
Stained
Intracellular HLA
Intracellular CXCR5
APC
D
Mean fluorescence intensity
40
30
20
10
0
*
-RTA
+RTA

Figure 9

A

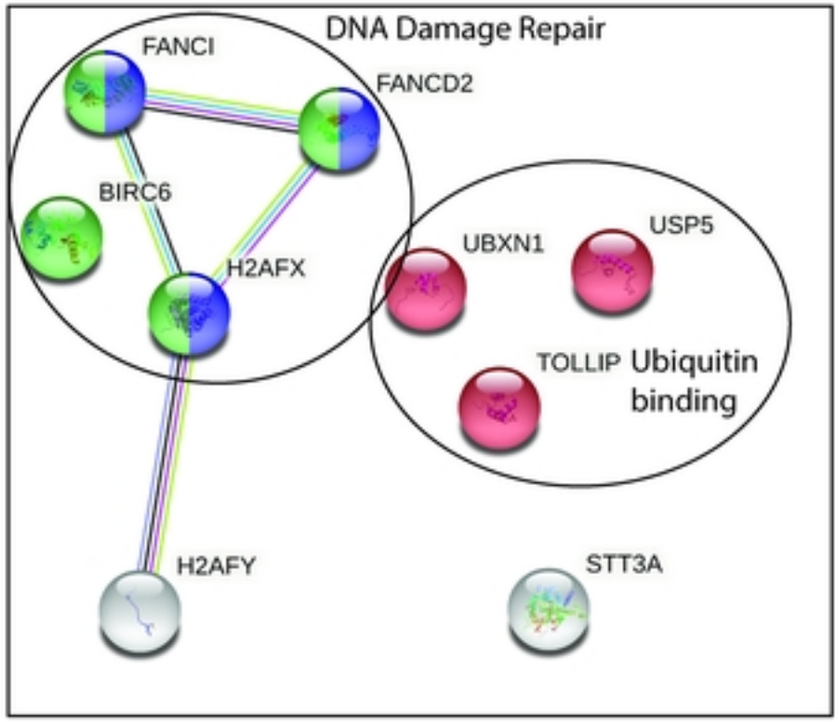

B

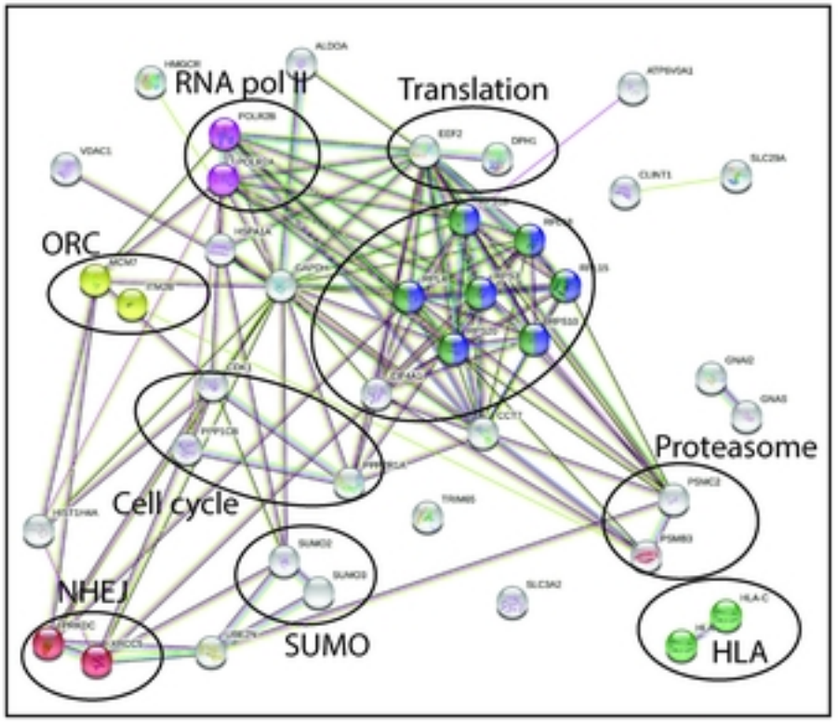

D

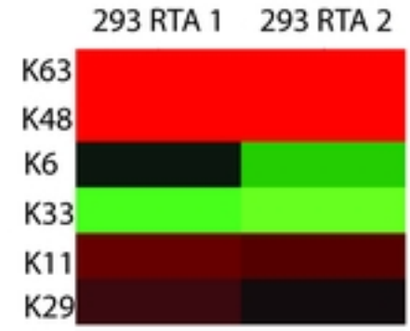

C

Decreased ubiquitination				
Term	Count	%	PValue	Benjamini
GO:0006334~nucleosome assembly	5	35.71	1.08E-06	1.36E-04
GO:0036297~interstrand cross-link repair	3	21.43	2.92E-04	0.01823456
GO:0006511~ubiquitin-dependent protein catabolic process	4	28.57	7.97E-04	0.03321451
Increased ubiquitination				
Term	Count	%	PValue	Benjamini
GO:0002181~cytoplasmic translation	8	13.79	8.40E-09	4.44E-07
GO:0006412~translation	8	13.79	4.11E-06	1.93E-04
GO:0007017~microtubule-based process	5	8.62	5.82E-06	2.46E-04
GO:0000226~microtubule cytoskeleton organization	6	10.34	4.74E-05	0.00182359
GO:0000278~mitotic cell cycle	5	8.62	0.00111799	0.03940899
GO:0030705~cytoskeleton-dependent intracellular transport	3	5.17	0.00142527	0.04637625

Figure 4